

Technical Report Documentation Page

1. Report No. FHWA/TX-04/0-4185-2	2. Government Accession No.	3. Recipient's Catalog No.	
4. Title and Subtitle HAMBURG WHEEL TRACKING DEVICE RESULTS ON PLANT AND FIELD CORES PRODUCED MIXTURES		5. Report Date September 2002	
		6. Performing Organization Code	
7. Author(s) Yetkin Yildirim, Thomas W. Kennedy		8. Performing Organization Report No. 0-4185-2	
9. Performing Organization Name and Address Center for Transportation Research The University of Texas at Austin 3208 Red River, Suite 200 Austin, TX 78705-2650		10. Work Unit No. (TRAIS)	
		11. Contract or Grant No. 0-4185	
12. Sponsoring Agency Name and Address Texas Department of Transportation Research and Technology Implementation Office P.O. Box 5080 Austin, TX 78763-5080		13. Type of Report and Period Covered Research Report	
		14. Sponsoring Agency Code	
15. Supplementary Notes Project conducted in cooperation with the U.S. Department of Transportation, Federal Highway Administration, and the Texas Department of Transportation.			
16. Abstract This project was conducted to determine the correlation of field performance to Hamburg Wheel Tracking Device (HWTD) testing results. HWTD measures the combined effects of rutting and moisture damage by rolling a steel wheel across the surface of an asphalt concrete specimen that is immersed in hot water. The test results from this laboratory equipment have been promising in regard to evaluating the moisture susceptibility of hot mix asphalt mixtures. While there is some information on the relationship between the laboratory results from this test and the field performance, it is quite limited. This 5-year research project will be an important step in validating the test and ensuring that the test results could be reliably used to predict performance. Three designs (Superpave, CMHB-C, and Type C) and three aggregate sources (siliceous gravel, sandstone, and quartzite) were used for this study. The test sections including nine different mixture designs were constructed on IH 20 in Harrison County to observe the performance of the overlays under real traffic conditions. Field performance will be observed through visual pavement condition surveys and non-destructive tests for four years. In the second year of this project, the samples from plant mixes and cores from the test sections were taken for each mixture type. The samples were tested using a HWTD by TxDOT's Flexible Pavements Branch of the Materials and Pavements Section of the Construction Division			
17. Key Words Hamburg Wheel Tracking Device (HWDT), Pavement Performance, Non-Destructive Testing		18. Distribution Statement No restrictions. This document is available to the public through the National Technical Information Service, Springfield, Virginia 22161.	
19. Security Classif. (of report) Unclassified	20. Security Classif. (of this page) Unclassified	21. No. of pages 72	22. Price

Hamburg Wheel Tracking Device Results on Plant and Field Cores Produced Mixtures

By

**Dr. Yetkin Yildirim, P.E.
Dr. Thomas W. Kennedy, P.E.**

Research Report 0-4185-2

Research Project 0-4185
Correlation of Field Performance to Hamburg Wheel Tracking Results

conducted for the
Texas Department of Transportation
in cooperation with
U.S. Department of Transportation
Federal Highway Administration
by the
Center for Transportation Research
Bureau of Engineering Research
The University of Texas at Austin

September 2002

Preface

This is the second report from the Center for Transportation Research (CTR) on Project 4185. This project is concerned with the investigation of the Hamburg Wheel Tracking Device test results to the field performance of the hot mix asphalt (HMA) mixture. This report presents the results and findings of the lab tests, and information collected from test sections for the second year of a 5-year project.

Acknowledgments

This project has been initiated and sponsored by the Texas Department of Transportation (TxDOT). The financial support of TxDOT is greatly appreciated. The authors would like to thank TxDOT Project Director Miles Garrison for his guidance. Special thanks are extended to Richard Izzo and Dale Rand of TxDOT for their great assistance in conducting the laboratory tests. The assistance of the Atlanta District personnel is greatly appreciated. We are also grateful to Soheil Nazarian and Deren Yuan for their perseverance in carrying forward and conducting the seismic pavement analyzer (SPA) testing.

Disclaimers

The contents of this report reflect the views of the authors, who are responsible for the facts and the accuracy of the data presented herein. The contents do not necessarily reflect the official views or policies of the Texas Department of Transportation (TxDOT). This report does not constitute a standard, specification, or regulation.

There was no invention or discovery conceived or first actually reduced to practice in the course of or under this contract, including any art, method, process, machine, manufacture, design or composition of matter, or any new and useful improvement thereof, or any variety of plant, which is or may be patentable under the patent laws of the United States of America or any foreign country.

NOT INTENDED FOR CONSTRUCTION, BIDDING, OR PERMIT PURPOSES

Dr. Yetkin Yildirim, P.E. (Texas No. 92787)

Dr. Thomas W. Kennedy, P.E. (Texas No. 29596)

Research Supervisors

Table of Contents

CHAPTER 1. INTRODUCTION	1
BACKGROUND	1
OBJECTIVE	2
SCOPE	3
CHAPTER 2. EXPERIMENTAL PROGRAM	5
TEST PLAN.....	5
MATERIALS AND MIXTURE DESIGNS.....	6
Superpave Mixes.....	6
CMHB-C Mixes.....	7
Type C Mixes.....	7
CHAPTER 3. TEST RESULTS	9
FIELD SPECIMENS	9
PLANT SPECIMENS.....	13
CHAPTER 4. VISUAL PAVEMENT CONDITION SURVEY.....	17
WEST BOUND OUTSIDE LANE.....	17
EAST BOUND OUTSIDE LANE.....	18
NONDESTRUCTIVE TESTING.....	18
CHAPTER 5. CONCLUSIONS	21
REFERENCES.....	23
APPENDIX A ANALYSES OF THE HAMBURG WHEEL TRACKING DEVICE	
DATA: RUT DEPTHS AT VARIOUS WHEEL PASSES	25
APPENDIX B PHOTOGRAPHS OF CRACKS AND POTHOLES OBSERVED ON	
THE WEST BOUND OUTSIDE LANE AND EAST BOUND OUTSIDE	
LANE	39
APPENDIX C AGGREGATE AND MIX DESIGN PROPERTIES OF THE	
SPECIMENS.....	51
APPENDIX D ORIENTATION OF THE TEST SECTIONS	57

List of Tables

Table 2.1 Test Plan for Surface Mixture Designs at Test Sections	5
Table 2.2 Test Plan for the HWTD Tests	6
Table 3.1 Rut Depths at Various Wheel Passes for Field Samples	10
Table 3.2 HWTD Indices for Field Samples	10
Table 3.3 Rut Depths at Various Wheel Passes for Plant Mix Samples	13
Table 3.4 HWTD Indices for Plant Mix Samples	14
Table 4.1 Visual Pavement Condition Survey Results at West Bound Outside Lane	17
Table 4.2 Beginning and Ending of the Test Sections at West Bound Outside Lane	17
Table 4.3 Visual Pavement Condition Survey Results at East Bound Outside Lane	18
Table 4.4 Beginning and Ending of the Test Sections at East Bound Outside Lane	18
Table C.1 Sources of the Materials Used in This Research Project	53
Table C.2 Aggregate Gradations for Superpave Mixes	53
Table C.3 Summary of Design Mixture Properties for Superpave Mixes	53
Table C.4 Aggregate Gradations for CMHB-C Mixes	54
Table C.5 Summary of Design Mixture Properties for CMHB-C Mixes	54
Table C.6 Aggregate Gradations for Type C Mixes	54
Table C.7 Summary of Stability, TSR, and HWTD Tests Results	55
Table D.1 Summary of Test Section, West Bound	59
Table D.2 Summary of Test Section, East Bound	59

List of Figures

Figure 3.1 Comparison of Superpave Field Mixes	11
Figure 3.2 Comparison of CMHB-C Field Mixes	12
Figure 3.3 Comparison of Type C Field Mixes	12
Figure 3.4 Comparison of Superpave Plant Mixes	15
Figure 3.5 Comparison of CMHB-C Plant Mixes	15
Figure 3.6 Comparison of Type C Plant Mixes	16
Figure A.1 Comparison of aggregate type effect on rut depth at 1,000 wheel passes for field samples	27
Figure A.2 Comparison of aggregate type effect on rut depth at 1,000 wheel passes for plant samples	27
Figure A.3 Comparison of aggregate type effect on rut depth at 5,000 wheel passes for field samples	28
Figure A.4 Comparison of aggregate type effect on rut depth at 5,000 wheel passes for plant samples	28
Figure A.5 Comparison of aggregate type effect on rut depth at 10,000 wheel passes for field samples	29
Figure A.6 Comparison of aggregate type effect on rut depth at 10,000 wheel passes for plant samples	29
Figure A.7 Comparison of aggregate type effect on rut depth at 15,000 wheel passes for field samples	30
Figure A.8 Comparison of aggregate type effect on rut depth at 15,000 wheel passes for plant samples	30
Figure A.9 Comparison of aggregate type effect on rut depth at 20,000 wheel passes for field samples	31
Figure A.10 Comparison of aggregate type effect on rut depth at 20,000 wheel passes for plant samples	31
Figure A.11 Comparison of aggregate type effect on creep slopes for field samples	32
Figure A.12 Comparison of aggregate type effect on creep slopes for plant samples	32
Figure A.13 Comparison of mix design effect on rut depth at 1,000 wheel passes for field samples	33
Figure A.14 Comparison of mix design effect on rut depth at 1,000 wheel passes for plant samples	33
Figure A.15 Comparison of mix design effect on rut depth at 5,000 wheel passes for field samples	34
Figure A.16 Comparison of mix design effect on rut depth at 5,000 wheel passes for plant samples	34
Figure A.17 Comparison of mix design effect on rut depth at 10,000 wheel passes for field samples	35
Figure A.18 Comparison of mix design effect on rut depth at 10,000 wheel passes for plant samples	35
Figure A.19 Comparison of mix design effect on rut depth at 15,000 wheel passes for field samples	36

Figure A.20 Comparison of mix design effect on rut depth at 15,000 wheel passes for plant samples.....	36
Figure A.21 Comparison of mix design effect on rut depth at 20,000 wheel passes for field samples	37
Figure A.22 Comparison of mix design effect on rut depth at 20,000 wheel passes for plant samples.....	37
Figure A.23 Comparison of mix design effect on creep slopes for field samples.....	38
Figure A.24 Comparison of mix design effect on creep slopes for plant samples.....	38
Figure B.1 Moderate transverse crack between 1305 – 1306	41
Figure B.2 Moderate transverse crack between 1300 – 1301	41
Figure B.3 Low transverse crack between 1296 – 1297	42
Figure B.4 Low transverse crack between 1292 – 1293	42
Figure B.5 Low transverse crack between 1250 – 1251	43
Figure B.6 Low transverse crack between 1245 – 1246	43
Figure B.7 Moderate transverse crack between 1234 – 1235	44
Figure B.8 Low transverse crack between 1228 – 1229	44
Figure B.9 Low transverse crack between 1223 – 1224	45
Figure B.10 Low transverse crack between 1210 – 1211	45
Figure B.11 Low transverse crack between 1215 – 1216	46
Figure B.12 Low transverse crack between 1195 – 1196	46
Figure B.13 Low pothole between 1150 – 1151	47
Figure B.14 Low pothole between 1249 – 1250	47
Figure B.15 Low pothole between 1238 – 1239	48
Figure B.16 Low pothole between 1288 – 1289	48
Figure B.17 Low transverse crack between 1292 – 1293	49
Figure D.1 Layout of the Test Sections	60

Chapter 1. Introduction

BACKGROUND

Maintenance is a significant issue in pavement construction affecting the service life and lifetime cost of a roadway. Proper and timely maintenance strategies can prolong the service life while reducing the cost of repairs. Asphalt overlays that can be applied on both flexible and rigid pavements are used as an effective way of maintenance.

This project was conducted to determine the correlation of field performance to Hamburg Wheel Tracking test results. Three designs (Superpave, CMHB-C, and Type C) and three aggregate sources (siliceous gravel, sandstone, and quartzite) were used for this study. The test sections, including all mixture designs, were constructed on IH 20 in Harrison County to observe the performance of the overlays under real traffic conditions. Type B mixture was used for all overlays as a base layer. Field performance will be observed through visual pavement condition surveys and nondestructive tests (NDT) for 4 years.

In the first year of Project 4185, specimens were prepared and tested using the Hamburg Wheel Tracking Device (HWTD). The results of the tests were analyzed and included in Research Report 4185-1 (1). In the second year of this project, samples from the plant mixes and cores from the test sections were taken for each mixture type. The samples were tested using the HWTD in the Texas Department of Transportation (TxDOT) asphalt laboratory. The HWTD is a wheel-tracking device used to simulate field traffic effects on hot mix asphalt pavement (HMA) in terms of rutting and moisture-induced damage (2). This equipment measures the combined effects of rutting and moisture damage by rolling a steel wheel across the surface of an asphalt concrete slab that is immersed in hot water. The HWTD was developed in the 1970s by Esso A.G. of Hamburg, Germany. Originally, only cubical-shaped specimens could be tested. The test now can be performed on both cubical and cylindrical specimens. The cubical specimens are approximately 320 mm long, 260 mm wide, and 40 mm thick. The cylindrical specimens are 150 to 300 mm in diameter and about 40 mm thick. The sample is typically compacted to 7±1 percent air voids. The plate type compactor has been proposed for compacting the specimens. However, use of cylindrical specimens makes it possible to obtain compacted specimens very easily with the aid of the gyratory compactors. Traditionally, the tests have been performed at 50 °C, even though the temperature can vary between 25 °C and 70 °C. Approximately 6.5 hours

are required for a test, but in many cases the samples have failed in a much shorter period of time (1). Specimens are tested in a submerged-in-water environment. The device operates two steel wheels simultaneously. Each wheel making about fifty passes per minute applies 705 ± 22 N force on specimens. Two samples are required for every single wheel. Because the device has two wheels, it can test four samples (two couples) at the same time and provides a single report for each couple. The test results from the HWTD include post-compaction consolidation, creep slope, stripping slope, stripping inflection point, and final rut depth (3). The post-compaction consolidation is the deformation (mm) at about 1,000 wheel passes. It is called post-compaction consolidation because it is assumed that the wheel is densifying the mixture within the first 1,000 wheel passes. The creep slope relates to rutting from plastic flow. It measures the accumulation of permanent deformation primarily owing to mechanisms other than moisture damage. The stripping slope is the inverse of the rate of deformation in the linear region of the deformation curve, after stripping begins and until the end of the test. This slope measures the accumulation of permanent deformation owing primarily to moisture damage. The stripping point is the number of passes at the intersection of the creep slope and the stripping slope. It is related to the resistance of the HMA to moisture damage. After this point, moisture damage starts to dominate performance. The Colorado Department of Transportation (CDOT) reports that an inflection point below 10,000 wheel passes indicates moisture susceptibility (2). To report the creep slope and the stripping slope in terms of wheel passes, inverse slopes are used. Higher creep slopes, stripping inflection points, and stripping slopes indicate less damage (4).

In this study, the HWTD data analyses were performed and the results are given in Chapter 3.

OBJECTIVE

The primary objective of this study is to determine the relationship between HMA field performance and the HWTD test results. Three mix designs (12.5 mm Superpave, CMHB-C, and Type C) and three different coarse aggregate types (siliceous gravel, sandstone, and quartzite) were studied in this project.

SCOPE

The project will be completed in 5 years. Test sections were built on IH 20 in Harrison County and nine different types of overlay were placed in December 2001. Test sections will be monitored for 4 years by the Center for Transportation Research (CTR) at The University of Texas at Austin. The HWTD was utilized to determine the laboratory performance of the samples. The HWTD results and the field performance of the overlays on continuously reinforced concrete pavement (CRCP) will be gathered and compared at the end of the project. The field performance will be observed using NDTs. Falling weight deflectometer (FWD), ground penetrating radar (GPR), portable seismic pavement analyzer (PSPA), and rolling dynamic deflectometer (RDD) are the types of NDT devices that will be utilized. In addition, visual pavement condition surveys will be performed at the end of each year. Field performance will be monitored every year until 2005. At the end of the project, the field and laboratory data will be compared to determine the behavior of the mixture types, and a guideline will be developed to correlate the HWTD results and field performance.

Chapter 2. Experimental Program

TEST PLAN

Nine hot mix asphalt (HMA) mixture types were prepared for this project using three mix designs: Type C, 12.5 mm Superpave, and CMHB-C mixture. Each mix design uses three different coarse aggregate sources: siliceous gravel, quartzite, and sandstone. Overlays were placed on test sections constructed on IH 20 in Harrison County. Test sections include all nine different types of surface mixtures shown in Table 2.1. The base course, which is the same for all surface mixtures, was designed with 90 percent limestone from Perch Hill and 10 percent field sand from Marshall. PG 76-22 binder was used for all mixtures including the base course.

Table 2.1 Test Plan for Surface Mixture Designs at Test Sections

	12.5 mm Superpave	CMHB-C	Type C
Gravel	1	1	1
Sandstone	1	1	1
Quartzite	1	1	1

Four specimens were prepared for each mix type given in Table 2.1, two of which come from the field and two from the plant mix. The specimens were tested in the TxDOT asphalt laboratory using the HWTD. The testing plan is shown in Table 2.2. Test results are given in Chapter 3.

Table 2.2 Test Plan for the HWTB Tests

	12.5 mm Superpave	CMHB-C	Type C
Gravel	4	4	4
Quartzite	4	4	4
Sandstone	4	4	4

MATERIALS AND MIXTURE DESIGNS

Siliceous gravel is made mostly of quartz-rich sand and sandstone. It shows high thermal expansion. Sandstone is a sedimentary rock that has quartz-rich varieties. If it is cemented by silica or iron oxides (feldspar, calcite, or clay), and it shows excellent quality. Sandstone is mostly porous and permeable. Pore water pressure plays a significant role in the compressive strength and deformation characteristics. It can reduce the unconfined compressive strength by 30 to 60 percent. Sandstone is resistant to surface wearing. It shows variable toughness, hardness and durability, good crushed shape, and excellent chemical stability and surface characteristics. It has relatively low density of 2.54 g/cm^3 . Quartzite is a metamorphic rock. It is made of quartz (silicon dioxide) and sandstone. It is one of the hardest, toughest, and most durable rocks known. Because it has a high quartz content, it requires an anti-stripping agent when used with bituminous materials. Quartzite is excellent in toughness, hardness, durability, and chemical stability, is fair in crushed shape, and is fair to good in surface characteristics. Its density is 2.69 g/cm^3 , which is medium.

The source of the binder was Wright Asphalt of Houston, Texas. Aggregates were obtained from different sources and locations. Aggregate source and location data are provided in Table C.1.

Superpave Mixes

A nominal maximum aggregate size of 12.5 mm was used for all three Superpave mixes designed for this project. The first Superpave mix is composed of 67 percent siliceous gravel, 32 percent limestone screenings, and 1 percent lime. The design asphalt binder content for this mix is 5.0 percent. The second Superpave mix is composed of 91 percent sandstone, 8 percent

igneous screenings, and 1 percent lime. The design asphalt binder content for this mix is 5.1 percent. The third Superpave mix is composed of 89 percent quartzite, 10 percent igneous screenings, and 1 percent lime. The design asphalt binder content is 5.1 percent. All three Superpave mix design gradations are passing below the Superpave restricted zone. Table C.2 shows the aggregate gradations for these mixes.

All of the Superpave mixes satisfy Superpave mixture design requirements. Because all of the Superpave mixes are 12.5 mm, a minimum of 14.0 percent voids in mineral aggregate (VMA) value was used as a criterion. Based on the expected traffic level, specification for voids filled with asphalt (VFA) is selected between 65 and 75 percent. Densification requirements at the initial number of gyrations and maximum number of gyrations are a maximum of 89.0 percent and 98.0 percent, respectively. An acceptable dust portion (DP) ranges from 0.6 to 1.2 for all Superpave mixtures. Table C.3 summarizes the design mixture properties for Superpave mixes at design binder contents.

CMHB-C Mixes

The first CMHB-C mix is composed of 79 percent siliceous gravel, 20 percent igneous screenings, and 1 percent lime. The second CMHB-C mix is composed of 87 percent quartzite, 12 percent igneous screenings, and 1 percent lime. The third CMHB-C mix is composed of 87 percent sandstone, 12 percent igneous screenings, and 1 percent lime. The design asphalt binder content is 4.7 percent for the first mix and 4.8 percent for the second and the third mixes. The aggregate gradations for these mixes are shown in Table C.4. The level of air void at design is 3.5 percent for all CMHB-C mixes. Table C.5 shows the volumetric properties for CMHB-C mixes.

Type C Mixes

The first Type C mix is composed of 61 percent siliceous gravel, 30 percent limestone screenings, 8 percent igneous screenings, and 1 percent lime. The second Type C mix is composed of 91 percent quartzite, 8 percent igneous screenings, and 1 percent lime. The third Type C mix is composed of 99 percent sandstone and 1 percent lime. The design asphalt binder contents for the mixtures are 4.4 percent, 4.6 percent, and 4.5 percent, respectively. Gradation for Type C mixtures is shown in Table C.6.

The results of stability, tensile strength ratio (TSR), and the HWTD tests are given in Table C.7. The lowest stability value was recorded as 41 on the A 0112 (H 01-09) Superpave mix, and the highest value is recorded as 51 on the A 0112 (H 01-08) Superpave mix. Stability tests were not conducted on the A 0115 (H 01-16) and A 0116 (H 01-17) mixes. The highest TSR value was recorded as 1.06 on the A 0118 (H 01-19) Type C mix, and the lowest value was recorded as 0.90 on the A 0119 (H 01-20) Type C mix. HWTD tests were conducted for 20,000 passes. The deformations recorded after 20,000 passes are also shown in Table C.7. The highest deformation observed was 3.1 on the A 0111 (H 01-07) Superpave mix, and the lowest deformation recorded was 1.4 on the A 0116 (H 01-17) CMHB-C mix.

Chapter 3. Test Results

Field and plant mix samples were tested at 50 °C using the HWTD. Field specimens were tested up to 20,000 wheel passes, while plant mix samples were tested up to 100,000. Data from the HWTD were plotted on sheets, and post-compaction points, rut depths, and creep slopes for each specimen were determined. None of the specimens showed stripping deformation, which is moisture-induced damage; therefore, no stripping inflection point (SIP) was observed. Because the SIP, stripping slope, and failure point data are missing, post-compaction points, rutting depths at various points, and creep slopes are the performance parameters used in this study. The post-compaction point is densification of asphalt mixture owing to initial trafficking. Rut depth at 1,000 wheel passes is generally used as the post-compaction point. Creep slope, which indicates rutting susceptibility, is the average number of passes for 1 mm deformation before the stripping starts to take place. Creep slope is found by drawing a line that best fits the deformation curve, ranging from the post-compaction point to the point where stripping starts. Because there is no stripping for the field and plant mix specimens, the creep slopes were obtained by drawing the lines between the post-compaction point and the final wheel pass. Rut depths at 1,000, 5,000, 10,000, 15,000, 20,000, 50,000, 75,000, and 100,000 passes (the last three are only for plant mixes) and creep slopes were compared.

FIELD SPECIMENS

Field specimens were tested with the HWTD at 50 °C. A rut depth of 12.5 mm, or 20,000 passes was specified as an ending point for the HWTD test for field specimens. Specimens provided only post-compaction point and creep slope information, but no stripping slope and no stripping inflection point. Therefore, comparisons were based only on post-compactions, rutting depths, and creep slopes. Rut depths at various wheel passes, post-compactions, and creep slopes for field mixtures are given in the following tables.

Table 3.1 Rut Depths at Various Wheel Passes for Field Samples

Mix ID	Binder Type	Aggregate Type	Rut Depth (mm)				
			Number of Wheel Passes				
			1,000	5,000	10,000	15,000	20,000
Superpave	PG76-22	Siliceous Gravel	3.06	5.05	6.14	6.91	7.99
		Sandstone	4.02	6.55	7.58	8.64	9.38
		Quartzite	2.44	3.56	4.08	4.32	4.63
CMHB-C		Siliceous Gravel	2.51	4.67	5.51	6.00	6.73
		Sandstone	5.71	10.30	14.00	17.28	-
		Quartzite	2.85	4.33	5.61	7.07	8.05
Type C		Siliceous Gravel	N/A	N/A	N/A	N/A	N/A
		Sandstone	1.49	2.41	3.06	3.48	3.65
		Quartzite	2.11	2.85	3.67	4.16	4.45

Table 3.2 HWTD Indices for Field Samples

Mix ID	Binder Type	Percentage of Crushed Aggregate (%)	HWTD Indices				
			Post - compaction (mm)	Creep Slope (Passes/mm)	Stripping Slope (Passes/mm)	SIP (Passes-mm)	
Superpave	PG76-22	Siliceous Gravel	3.06	4,474	N/A	N/A	N/A
		Sandstone	4.02	4,368	N/A	N/A	N/A
		Quartzite	2.44	12,245	N/A	N/A	N/A
CMHB-C		Siliceous Gravel	2.51	6,259	N/A	N/A	N/A
		Sandstone	5.71	1,220	N/A	N/A	N/A
		Quartzite	2.85	3,823	N/A	N/A	N/A
Type C		Siliceous Gravel	N/A	N/A	N/A	N/A	N/A
		Sandstone	1.49	10,172	N/A	N/A	N/A
		Quartzite	2.11	8,348	N/A	N/A	N/A

Quartzite exhibited the best performances among three Superpave mix types in terms of rut depths and creep slopes. Siliceous gravel showed slightly better results than quartzite, while sandstone exhibited the worst results for CMHB-C mixes. Sandstone showed slightly better results than quartzite when used in Type C mix. Siliceous gravel Type C mix data are missing, thus these data could not be compared with the others. Siliceous gravel aggregate performs best when CMHB-C mix design is used. Type C design seems to be the most suitable mix design for sandstone, and Type C and Superpave designs are the best ones for quartzite. (Type C is slightly better.)

Superpave quartzite mix may seem to be the best-performing specimen among all nine specimens, if only creep slopes were taken into consideration, as shown in the following figure. Considering all indices together, Type C sandstone exhibits the best results. The higher creep slope of the Superpave quartzite specimen stems from high post compaction. The specimen shows very high compaction at the beginning; hence, the rutting rate slows down through the end of the test. The Superpave quartzite specimen always has higher rut depths throughout the test. Type C quartzite and Superpave quartzite are the second- and third- best specimens, respectively. CMHB-C sandstone is the worst-performing specimen, and it is followed by Superpave sandstone. Comparisons are shown in the figures below:

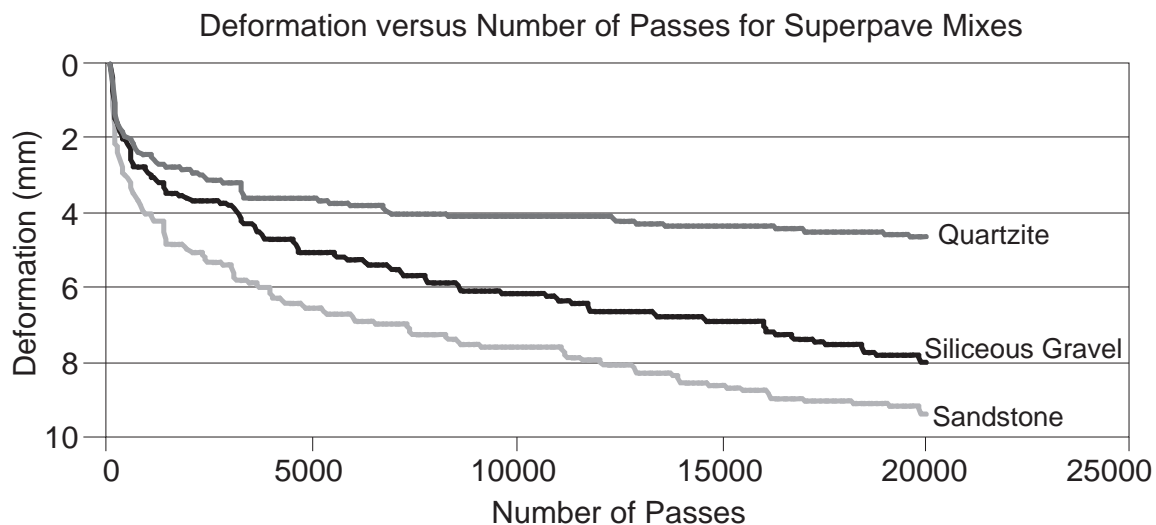


Figure 3.1 Comparison of Superpave Field Mixes

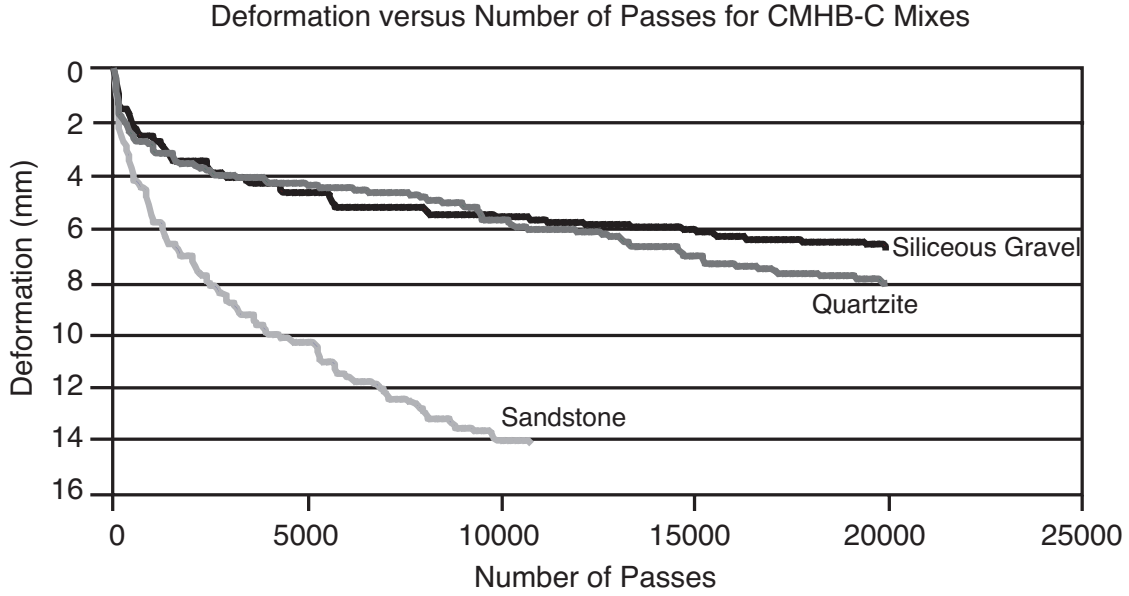


Figure 3.2 Comparison of CMHB-C Field Mixes

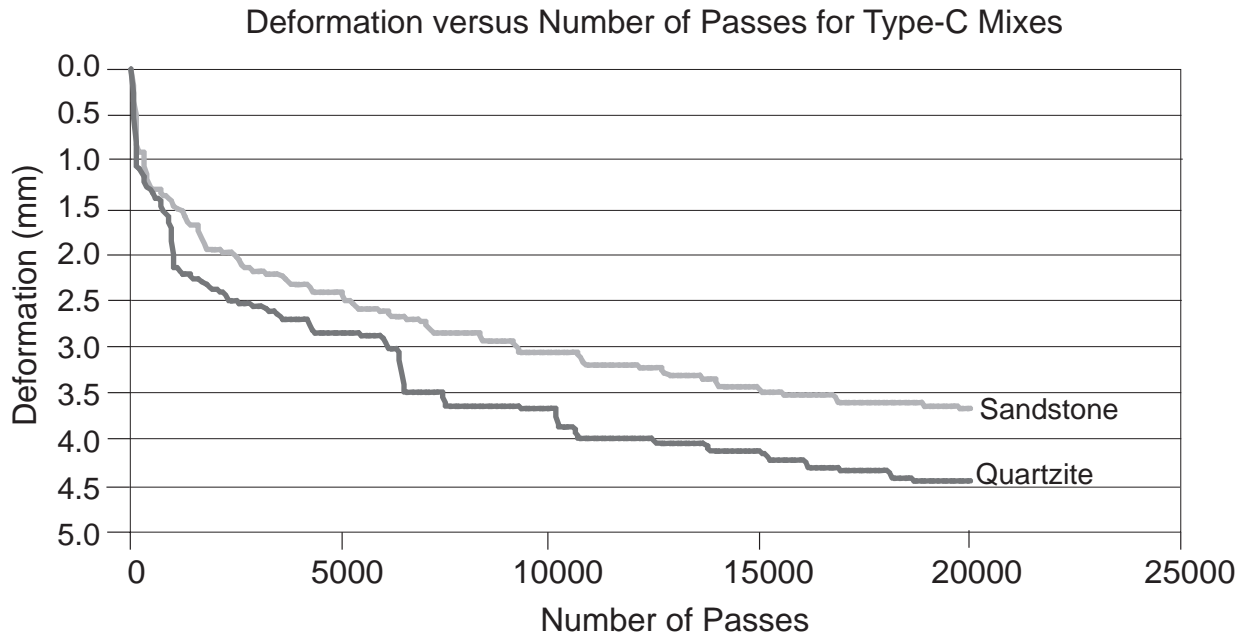


Figure 3.3 Comparison of Type C Field Mixes

PLANT SPECIMENS

Plant mix samples were tested for failure using the criteria of 12.5 mm or 100,000 passes. Specimens were tested at 50° C. Samples did not show any stripping slope, stripping inflection point, or failure. Indices and rutting depths are given in Table 3.3 and Table 3.4.

Table 3.3 Rut Depths at Various Wheel Passes for Plant Mix Samples

Mix ID	Binder Type	Aggregate Type	Rut Depth (mm)							
			Number of Wheel Passes							
			1,000	5,000	10,000	15,000	20,000	50,000	75,000	100,000
Superpave	PG76-22	Siliceous Gravel	0.64	1.50	1.64	1.84	1.99	2.85	3.45	3.82
		Sandstone	1.38	1.69	1.92	1.96	2.07	2.89	3.26	4.08
		Quartzite	1.50	2.04	2.42	3.04	3.43	4.05	4.41	4.69
CMHB-C		Siliceous Gravel	2.19	3.73	4.77	5.40	5.69	7.38	7.93	8.35
		Sandstone	1.06	1.38	1.52	1.63	1.76	2.09	2.29	2.43
		Quartzite	1.29	2.06	2.42	2.94	3.04	3.91	3.96	4.24
Type C		Siliceous Gravel	2.06	3.92	5.06	5.83	6.53	9.24	10.1	11.3
		Sandstone	0.95	1.24	1.27	1.27	1.30	1.36	1.39	1.43
		Quartzite	1.25	1.55	1.64	1.73	1.79	2.19	2.44	2.66

Table 3.4 HWTD Indices for Plant Mix Samples

Mix ID	Binder Type	Percentage of Crushed Aggregate (%)	HWTD Indices				
			Post - compaction (mm)	Creep Slope (Passes/mm)	Stripping Slope (Passes/mm)	SIP (Passes-mm)	
Superpave	PG76-22	Siliceous Gravel	1.55	62,224	N/A	N/A	N/A
		Sandstone	1.69	37,933	N/A	N/A	N/A
		Quartzite	1.79	43,185	N/A	N/A	N/A
CMHB-C		Siliceous Gravel	2.85	23,840	N/A	N/A	N/A
		Sandstone	1.14	93,209	N/A	N/A	N/A
		Quartzite	1.71	49,494	N/A	N/A	N/A
Type C		Siliceous Gravel	2.74	14,738	N/A	N/A	N/A
		Sandstone	1.05	479,046	N/A	N/A	N/A
		Quartzite	1.4	85,703	N/A	N/A	N/A

All plant mix samples exhibited better results than the field samples. Although the samples were tested up to 100,000 wheel passes, they did not show any stripping, or even any significant deformation. Siliceous gravel, sandstone, and quartzite gave the best results, respectively, for the Superpave mix design. However, siliceous gravel performed worst with the CMHB-C and the Type C mixes. The CMHB-C and the Type C design mixes were found to perform best when sandstone aggregate was used. Superpave is the most appropriate mix design when siliceous gravel is used as a coarse aggregate. Type C seems to be the most suitable mix design if sandstone or quartzite are chosen. Performances of different aggregates for different mix designs are given in the following figures.

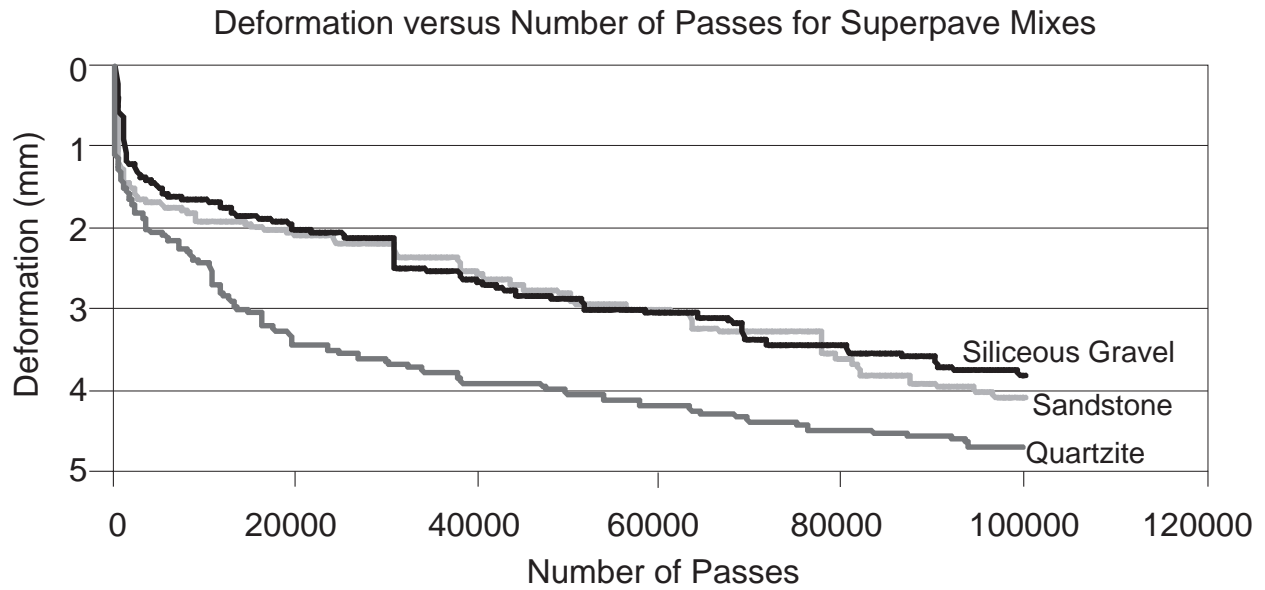


Figure 3.4 Comparison of Superpave Plant Mixes

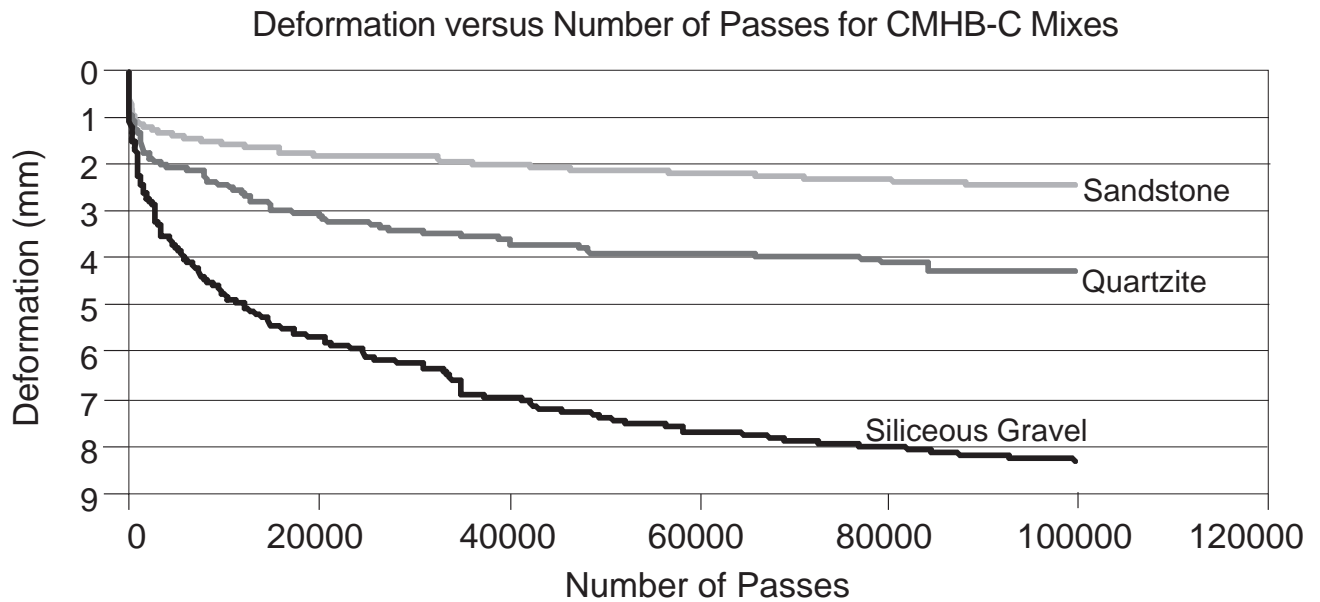


Figure 3.5 Comparison of CMHB-C Plant Mixes

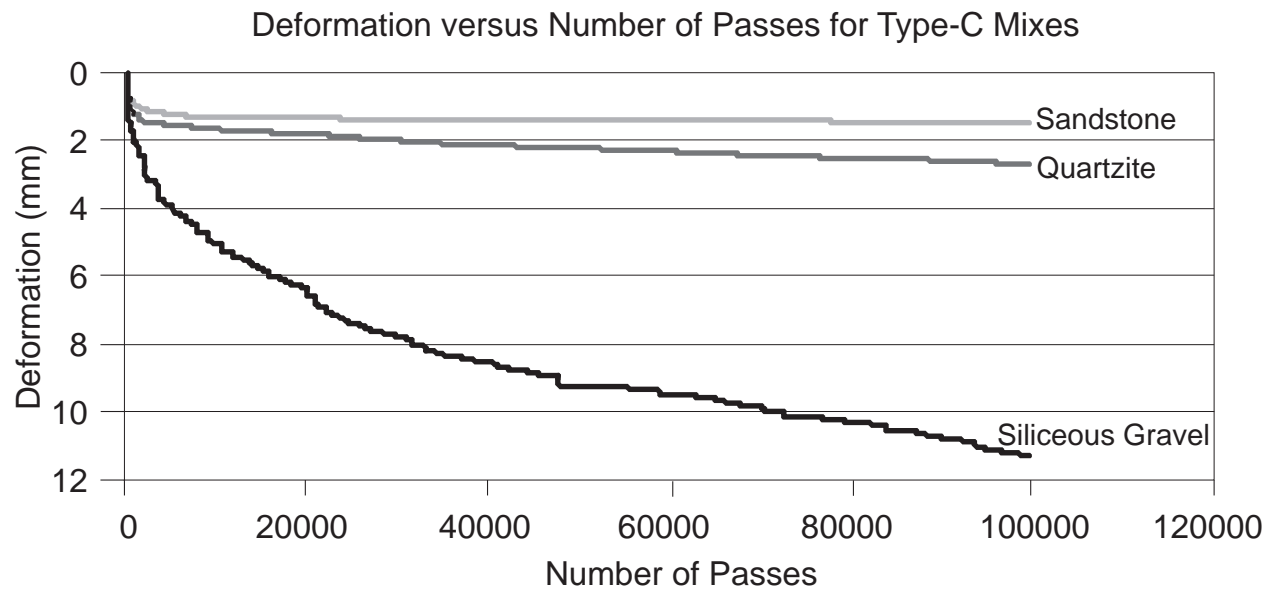


Figure 3.6 Comparison of Type C Plant Mixes

The Type C sandstone specimen shows the best results among all specimens, while Type C siliceous gravel seems to be the worst specimen. CMHB-C sandstone, which performs almost the same with the Type C quartzite specimen, follows Type C sandstone. Sandstone shows very high performance with all kinds of mixes. Quartzite also gave reasonable results with all three designs, especially Type C.

Chapter 4. Visual Pavement Condition Survey

WEST BOUND OUTSIDE LANE

West Bound Outside Lane was visited on 01/08/02. Distresses detected were mostly transverse cracking. Cracks were low- and moderate-level cracks, so they were considered to be insignificant. Visual condition survey results are given in Table 4.1.

Table 4.1 Visual Pavement Condition Survey Results at West Bound Outside Lane

Station Numbers	Distresses	Photo #
1305 - 1306	1 Moderate Transverse crack	Figure B1
1300 - 1301	1 Moderate Transverse crack	Figure B2
1296 - 1297	1 Low Transverse crack	Figure B3
1292 - 1293	1 Low Transverse crack	Figure B4
1250 - 1251	1 Low Transverse crack	Figure B5
1245 - 1246	1 Low Transverse crack	Figure B6
1242 - 1245	6 Low Transverse crack	Potters Creek Bridge
1234 - 1235	1 Moderate Transverse crack	Figure B7
1228 - 1229	1 Low Transverse crack	Figure B8
1223 - 1224	1 Low Transverse crack	Figure B9
1210 - 1211	1 Low Transverse crack	Figure B10
1215 - 1216	1 Low Transverse crack	Figure B11
1195 - 1196	1 Low Transverse crack	Figure B12
1150 - 1151	2 Low Pothole	Figure B13

Pictures of distresses are included in Appendix B. At least one picture for each crack was taken. Appendix B includes photos for cracks on the sections given in Table 4.1. Section station numbers and corresponding mixture and aggregate types are given in Table 4.2.

Table 4.2 Beginning and Ending of the Test Sections at West Bound Outside Lane

Station Numbers	Mixture Type	Aggregate
1278 - 1321	Superpave	Sandstone
1235 - 1278	CMHB-C	Sandstone
1193 - 1235	Type C	Sandstone
1135 - 1188	Superpave	Quartzite

EAST BOUND OUTSIDE LANE

East Bound Outside Lane was visited on 01/09/02. Low potholes and one low-level transverse crack were observed. Distresses were insignificant, so no correlation with laboratory tests could be done. Distresses are summarized in Table 4.3. Pictures of all distresses are available in Appendix B. The beginning and ending of the test sections and corresponding mixture and aggregate types are given in Table 4.4.

Table 4.3 Visual Pavement Condition Survey Results at East Bound Outside Lane

Station Numbers	Distresses	Photo #
1249 - 1250	Low Pothole	Figure B14
1238 - 1239	Low Pothole	Figure B15
1288 - 1289	Low Pothole	Figure B16
1292 - 1293	1 Low Transverse crack	Figure B17

Table 4.4 Beginning and Ending of the Test Sections at East Bound Outside Lane

Station Numbers	Mixture Type	Aggregate
1135 – 1185	CMHB–C	Quartzite
1190 – 1218	Type C	Quartzite
1218 – 1245	Superpave	Gravel
1245 - 1285	CMHB–C	Gravel
1282 - 1321	Type C	Gravel

NONDESTRUCTIVE TESTING

Seismic pavement analyzer (SPA) data could not be collected because the equipment was broken. Nondestructive Test (NDT), falling weight deflectometer (FWD), ground-penetrating radar (GPR), portable seismic pavement analyzer (PSPA), and rolling dynamic deflectometer (RDD) data were collected. Throughout the data collection process, there was a considerable amount of variation in the temperature of the pavement. Therefore, data should be calibrated based on the temperature differences. FWD data were collected by the Texas Department of Transportation (TxDOT), RDD data were collected by the University of Texas at Austin, and PSPA data were collected by the University of Texas at El Paso. Testing continued for 2 days

and only West Bound Outside and East Bound Outside lanes were tested. NDT data have not been analyzed in detail, so they are not included in the report.

Chapter 5. Conclusions

The primary objective of this project is to determine the effectiveness of the Hamburg Wheel Tracking Device (HWTd) in predicting the field performance of hot mix asphalt (HMA) mixtures. In this project, Superpave, CMHB-C, and Type C mix designs and siliceous gravel, sandstone, and quartzite aggregates were used. PG 76-22 asphalt binder was used for all mixtures. The project progressed in two phases, field and laboratory. Test sections were constructed in Harrison County to determine the field performances. Nine asphalt mixes with underlying Type B base mixture were placed on the test sections on IH 20 in Harrison County. Laboratory tests were conducted using the HWTd.

The HWTd test result analyses showed that among all the parameters, rut depth is of significant importance. Creep slope could not be taken as the only criterion when evaluating the HWTd test results. Analysis of rut depths at various points gives an accurate idea about how the other parameters, e.g., creep slope, were developed. Sometimes, high post-compaction may result in high creep slope, as in the case of the Superpave quartzite field specimen. However, rutting data show that this specimen has higher rut depths throughout the test. High creep slope is attributed to high post-compaction; hence, all the parameters, including post-compaction and rut depth at the end of the test, need to be analyzed when assessing the specimens.

The HWTd test results on both field cores and plant mix specimens indicate that in most cases, Type C sandstone mixture is superior to the other mixtures. The HWTd test results for field specimens designate Type C quartzite as the second-best mixture, while the HWTd test results for plant mix specimens indicate Type C quartzite as the third best-performing mixture. Mixtures with Type C design, except Type C siliceous gravel, gave sound results. Plant mix data shows that sandstone performs very well with all three mix designs, while field mix results show that sandstone mixes are the poorest ones, excluding Type C sandstone mix, which was found to be the best-performing specimen.

The project was scheduled to continue for 5 years. During this period field performances will be monitored using nondestructive devices, falling weight deflectometer (FWD), ground penetrating radar (GPR), portable seismic pavement analyzer (PSPA), and rolling dynamic deflectometer (RDD), and visual surveys will be carried out. The laboratory tests were already completed and the data was analyzed in this project. Performance of each mix design with three

aggregate types and performance of each aggregate source with three mix designs were evaluated. At the end of 5 years, all information from field and laboratory tests will be assembled and compared. It will then be determined if the HWTD could properly predict the performance of the overlays under field conditions, and the correlations will be developed between the HWTD and the field performance data.

References

1. Yildirim, Y. and T. W. Kennedy, "Correlation of Field Performance to Hamburg Wheel Tracking Device Results." Center for Transportation Research, Research Report 0-4185-1, October 2001.
2. Aschenbrener, T. and G. Currier, "*Influence of Testing Variables on the Results from the Hamburg Wheel Tracking Device*," Colorado Department of Transportation, CDOT-DTD-R-93-22, 1993.
3. Hines, M., "*The Hamburg Wheel Tracking Device*," Proceedings of the Twenty-Eight Paving and Transportation Conference, Civil Engineering Department, University of New Mexico, Albuquerque, New Mexico, 1991.
4. Mogawer, W. S., and K. D. Stuart, "*Effect of Coarse Aggregate Content on Stone Matrix Asphalt*," Transportation Research Record 1492, TRB, National Research Council, Washington, D.C., Pages 1-11, January 1995.

Appendix A

Analyses of the Hamburg Wheel Tracking Device Data: Rut Depths at Various Wheel Passes

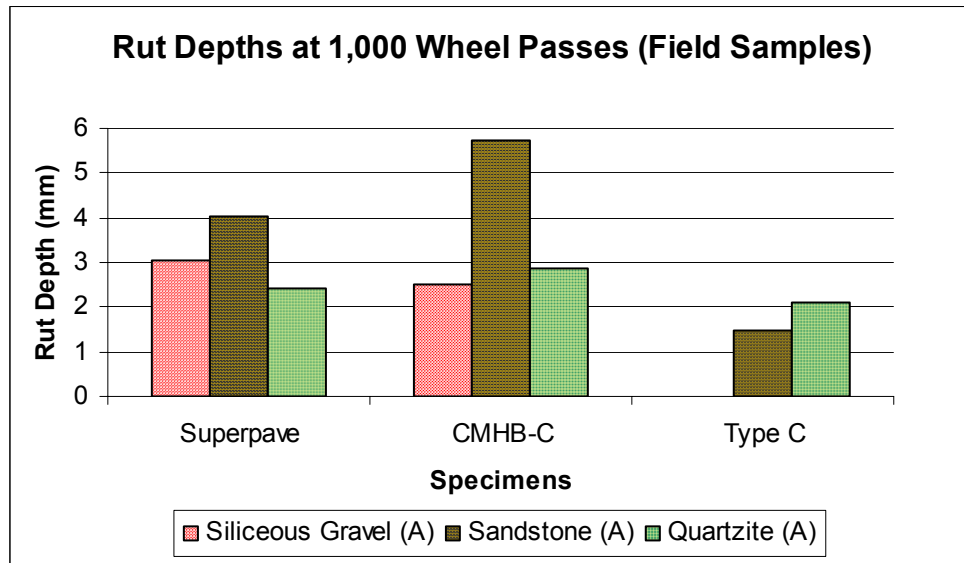


Figure A.1 Comparison of aggregate type effect on rut depth at 1,000 wheel passes for field samples

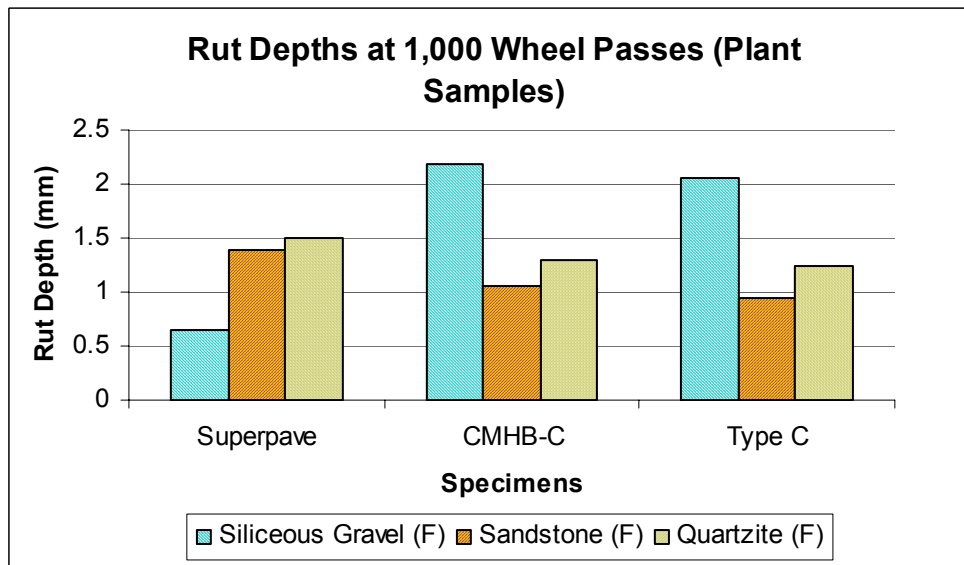


Figure A.2 Comparison of aggregate type effect on rut depth at 1,000 wheel passes for plant samples

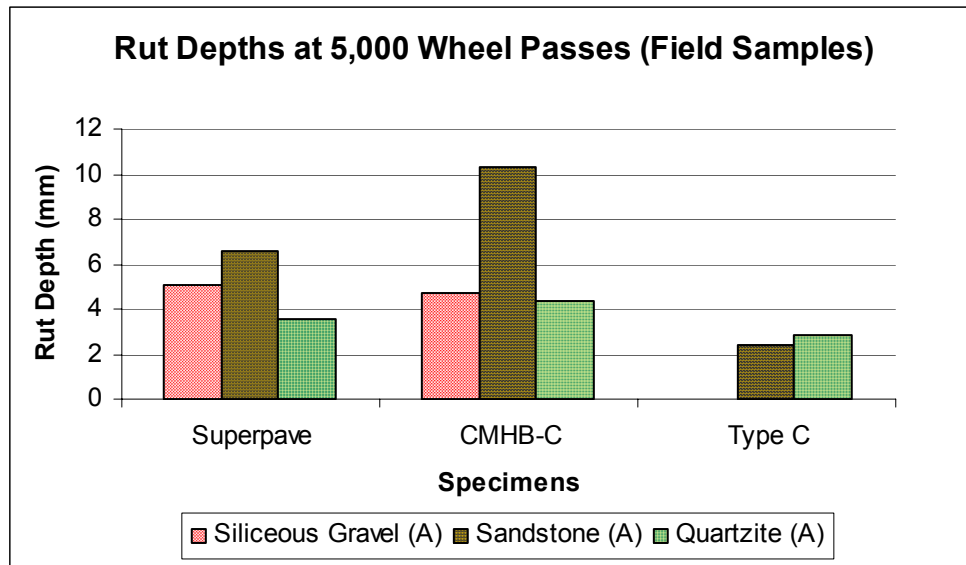


Figure A.3 Comparison of aggregate type effect on rut depth at 5,000 wheel passes for field samples

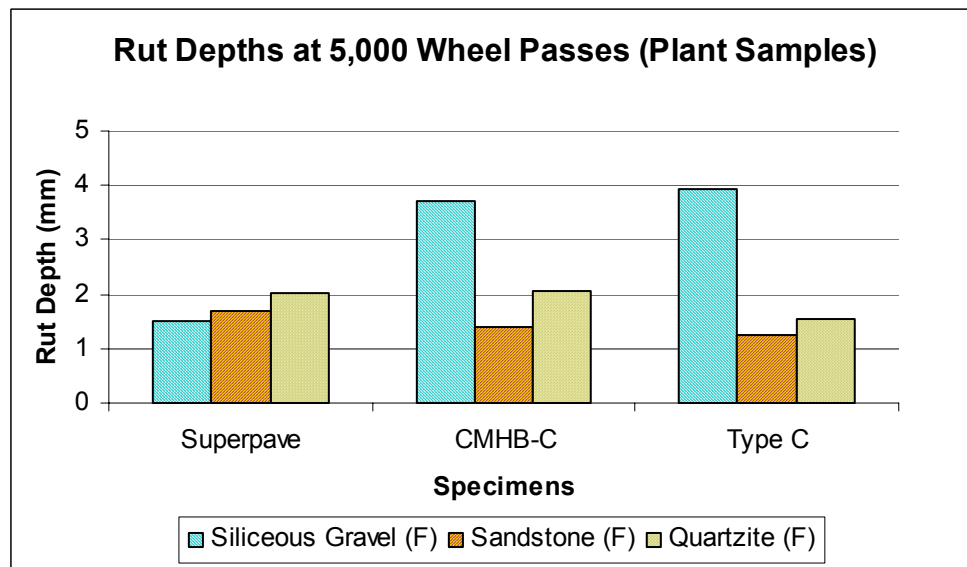


Figure A.4 Comparison of aggregate type effect on rut depth at 5,000 wheel passes for plant samples

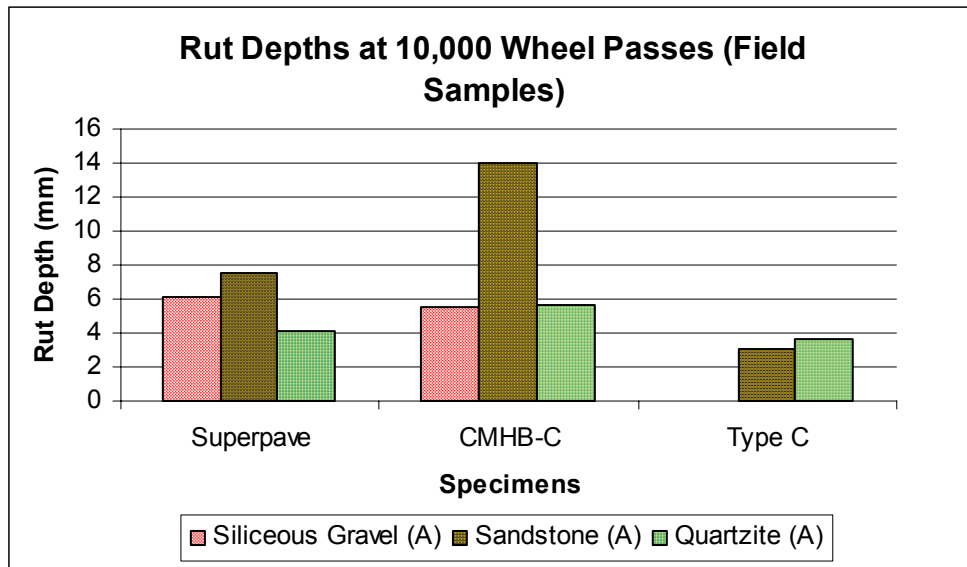


Figure A.5 Comparison of aggregate type effect on rut depth at 10,000 wheel passes for field samples

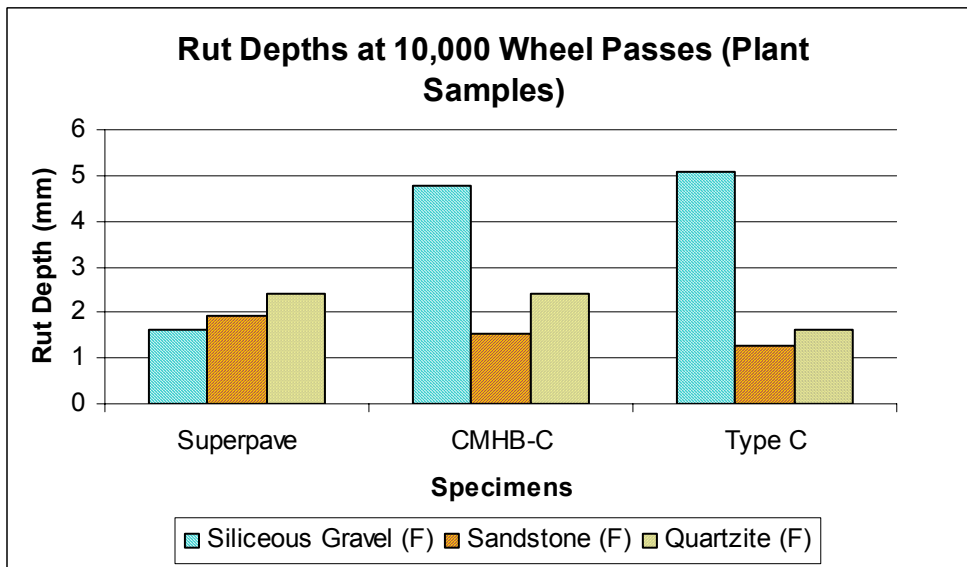


Figure A.6 Comparison of aggregate type effect on rut depth at 10,000 wheel passes for plant samples

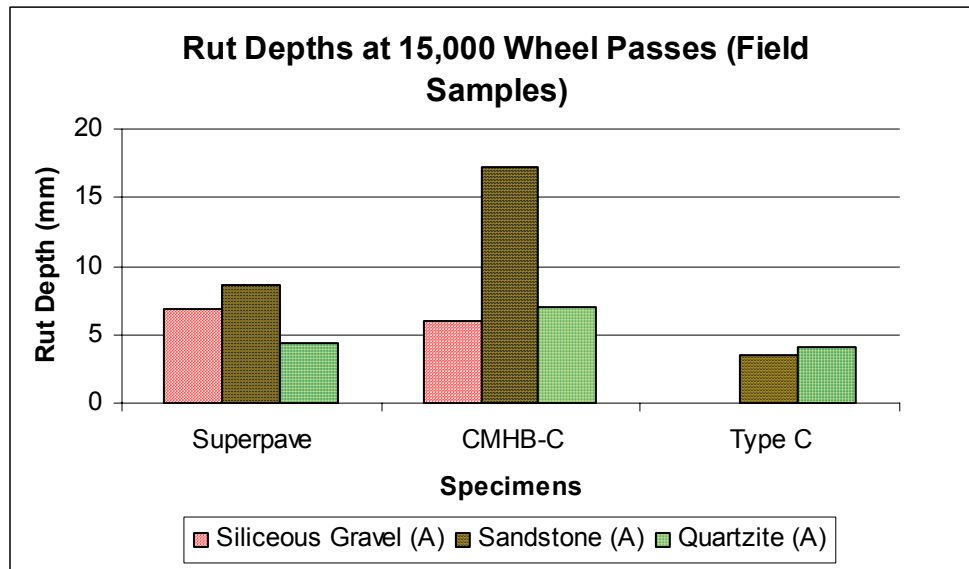


Figure A.7 Comparison of aggregate type effect on rut depth at 15,000 wheel passes for field samples

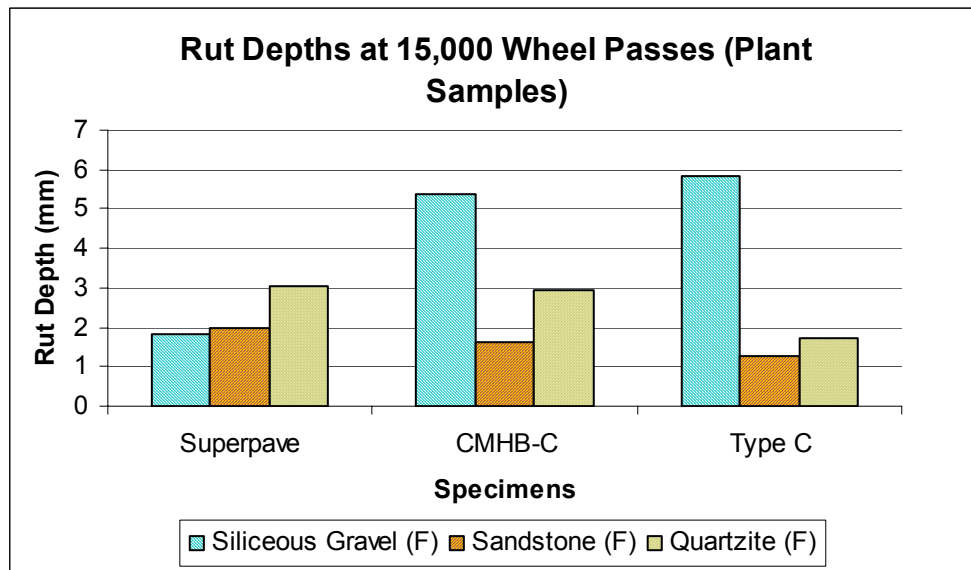


Figure A.8 Comparison of aggregate type effect on rut depth at 15,000 wheel passes for plant samples

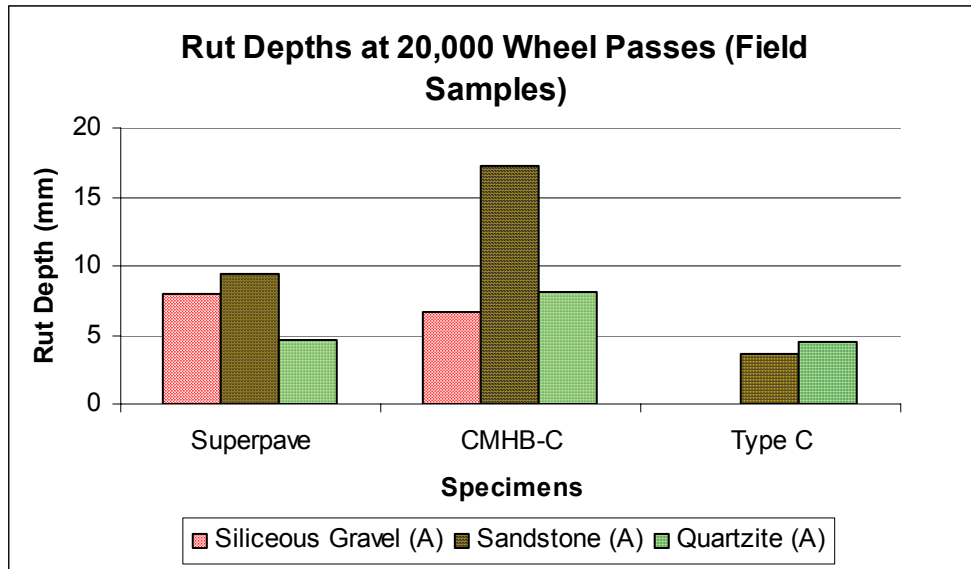


Figure A.9 Comparison of aggregate type effect on rut depth at 20,000 wheel passes for field samples

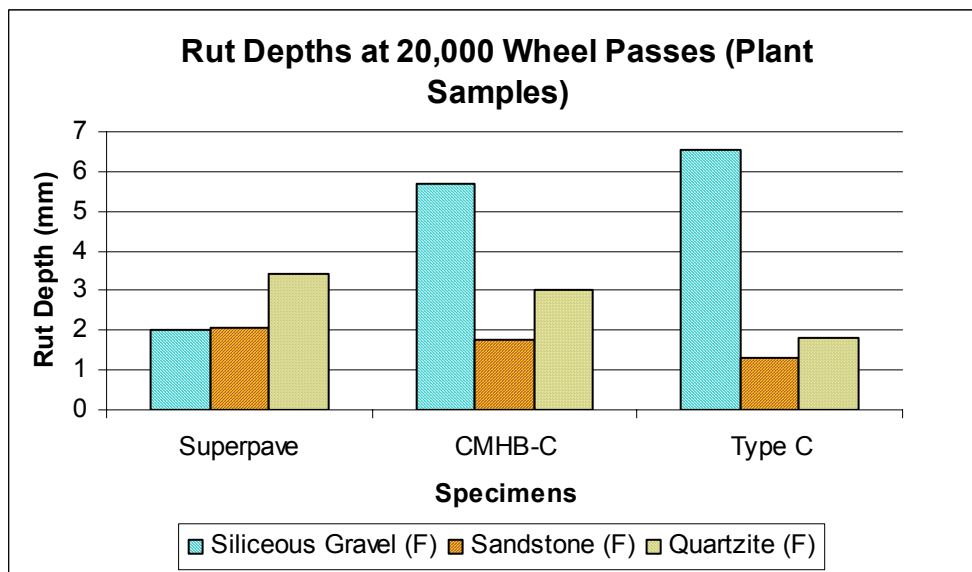


Figure A.10 Comparison of aggregate type effect on rut depth at 20,000 wheel passes for plant samples

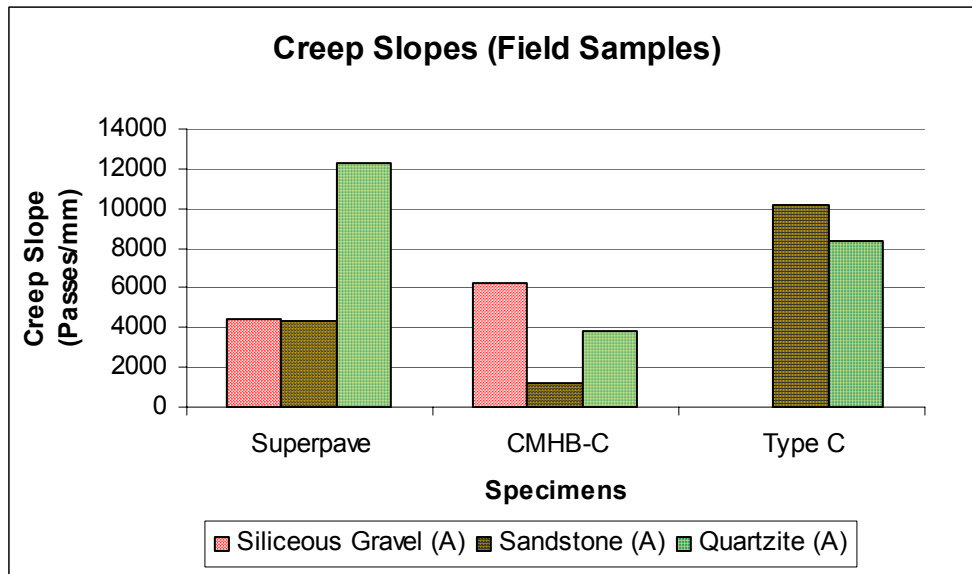


Figure A.11 Comparison of aggregate type effect on creep slopes for field samples

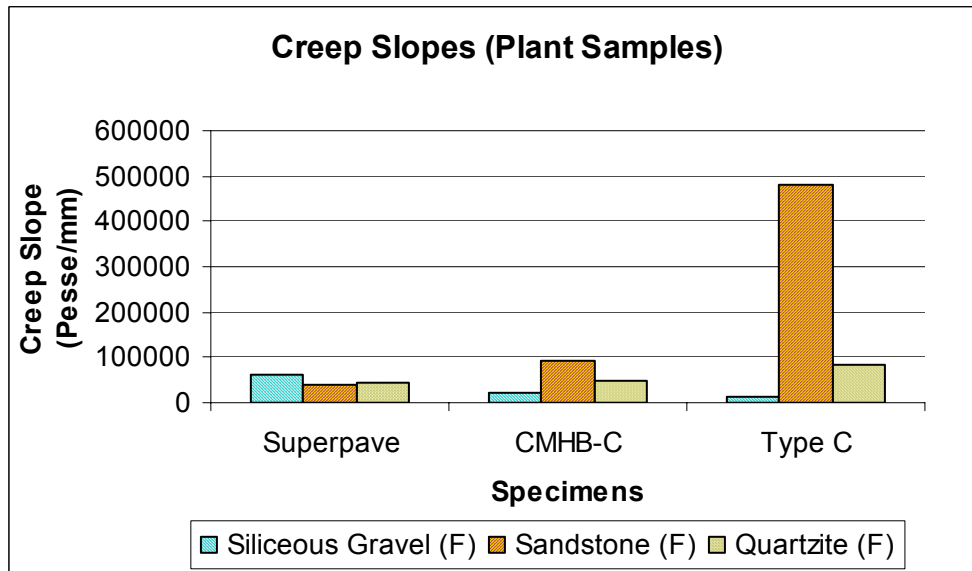


Figure A.12 Comparison of aggregate type effect on creep slopes for plant samples

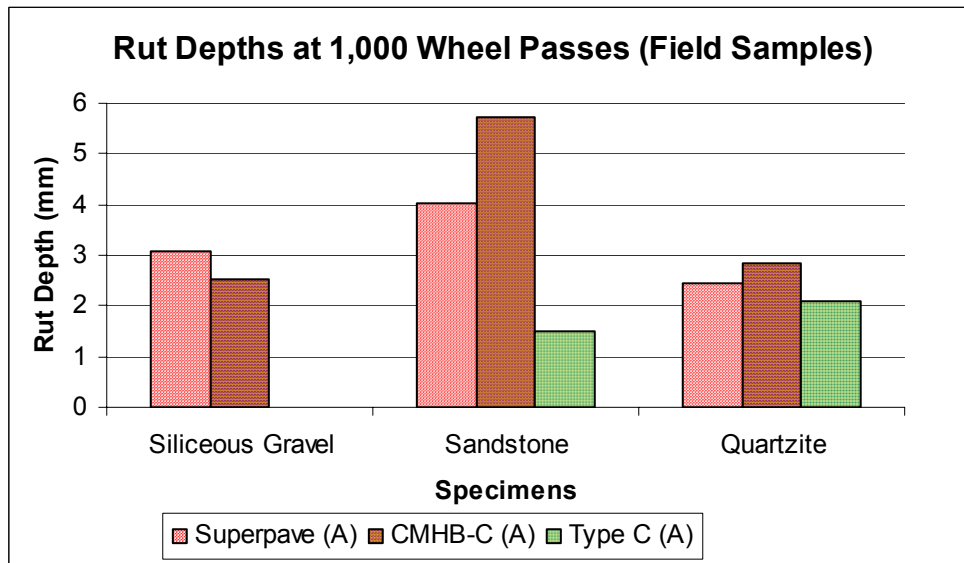


Figure A.13 Comparison of mix design effect on rut depth at 1,000 wheel passes for field samples

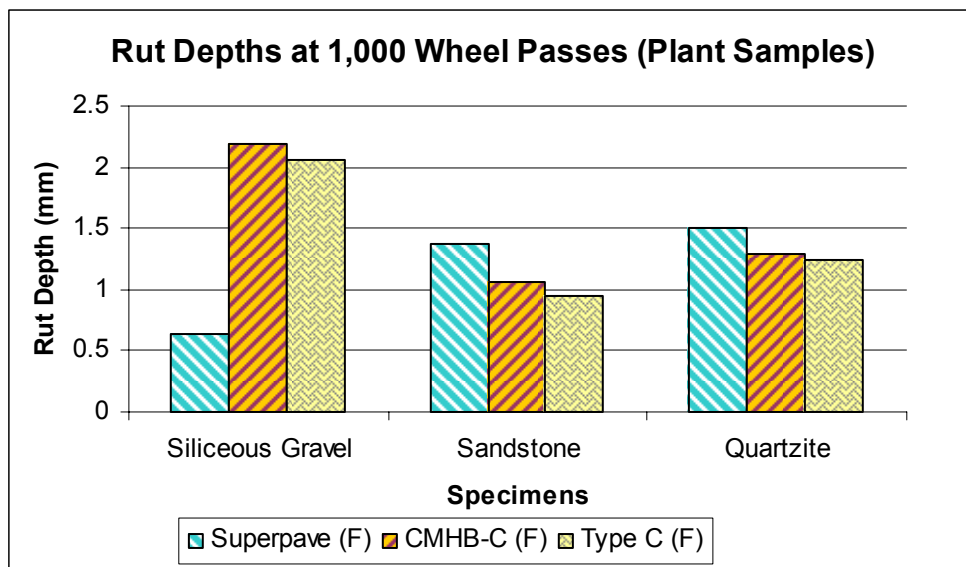


Figure A.14 Comparison of mix design effect on rut depth at 1,000 wheel passes for plant samples

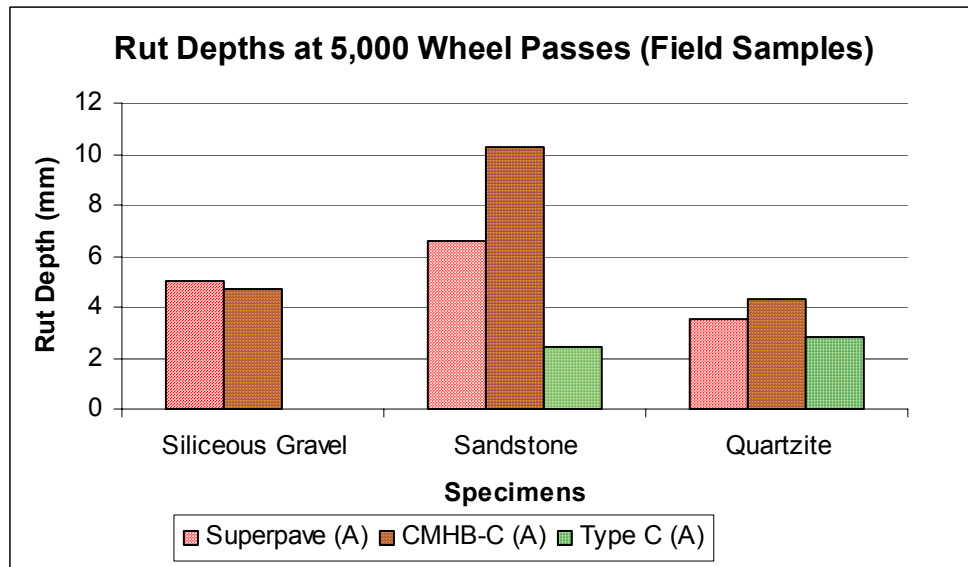


Figure A.15 Comparison of mix design effect on rut depth at 5,000 wheel passes for field samples

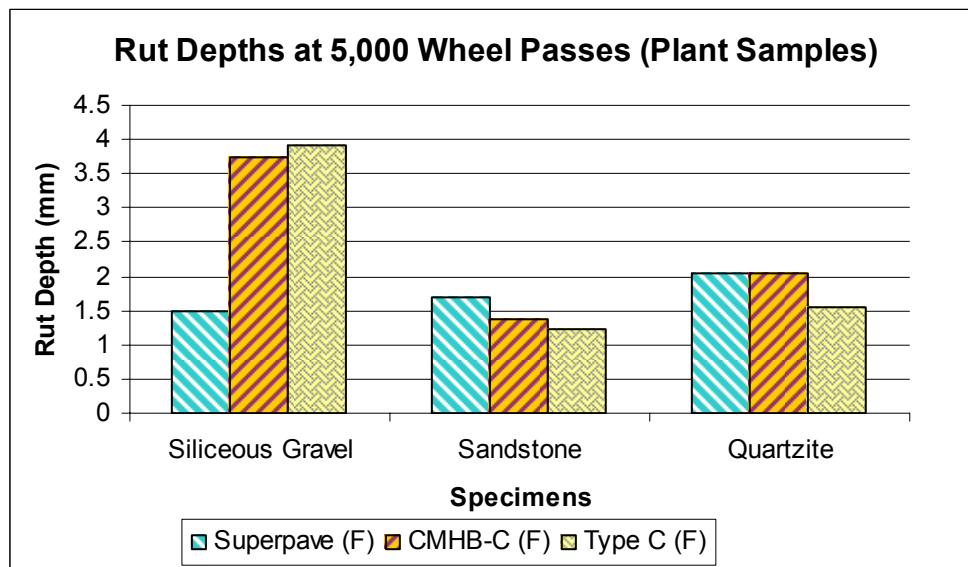


Figure A.16 Comparison of mix design effect on rut depth at 5,000 wheel passes for plant samples

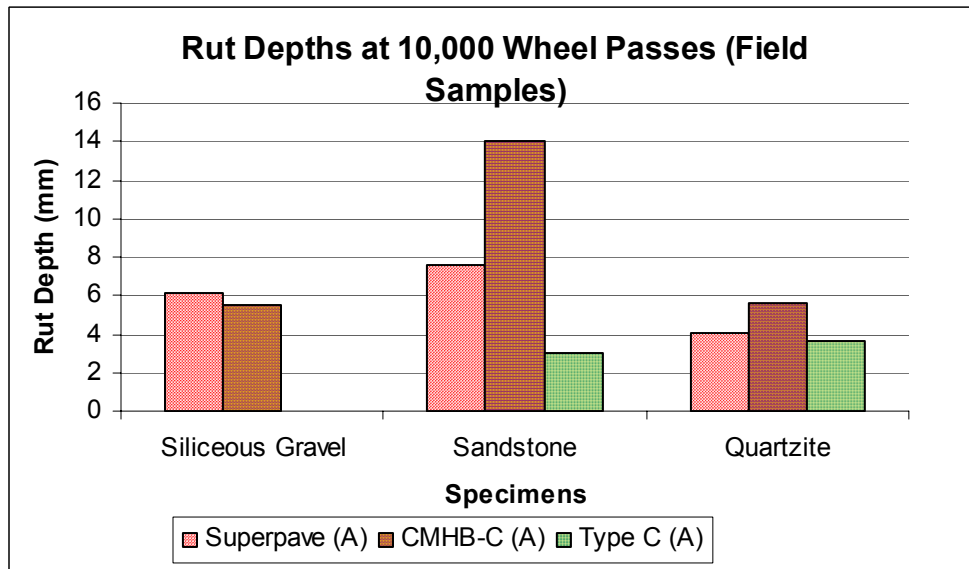


Figure A.17 Comparison of mix design effect on rut depth at 10,000 wheel passes for field samples

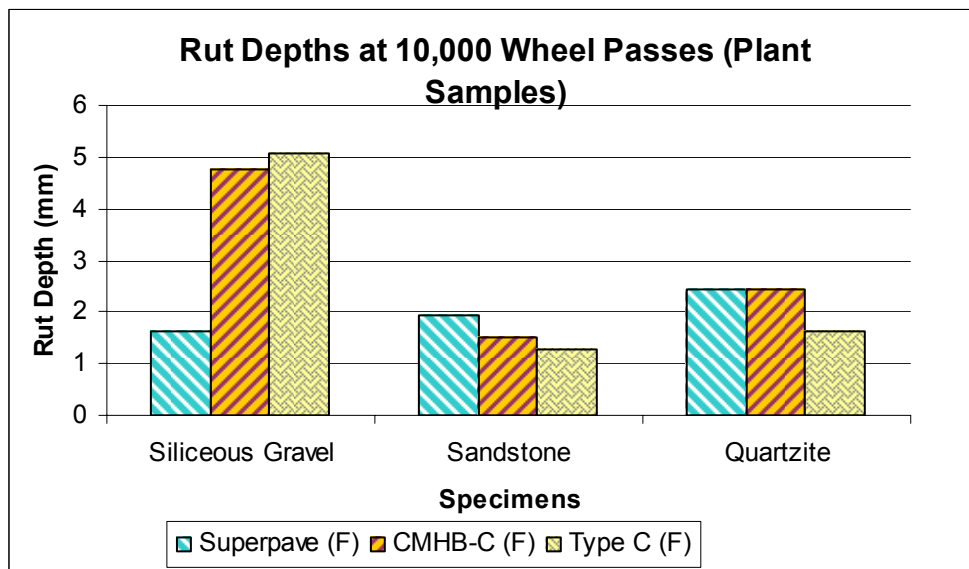


Figure A.18 Comparison of mix design effect on rut depth at 10,000 wheel passes for plant samples

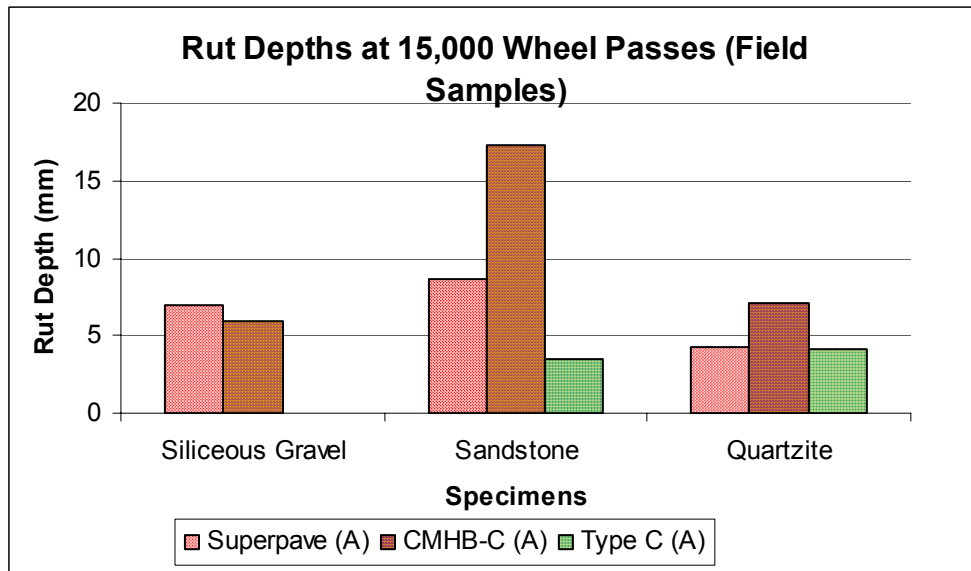


Figure A.19 Comparison of mix design effect on rut depth at 15,000 wheel passes for field samples

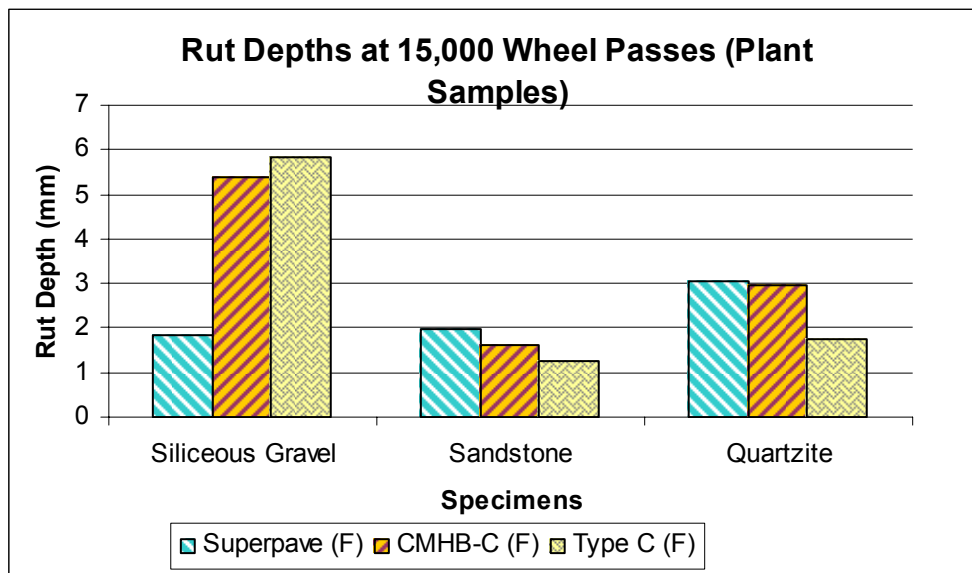


Figure A.20 Comparison of mix design effect on rut depth at 15,000 wheel passes for plant samples

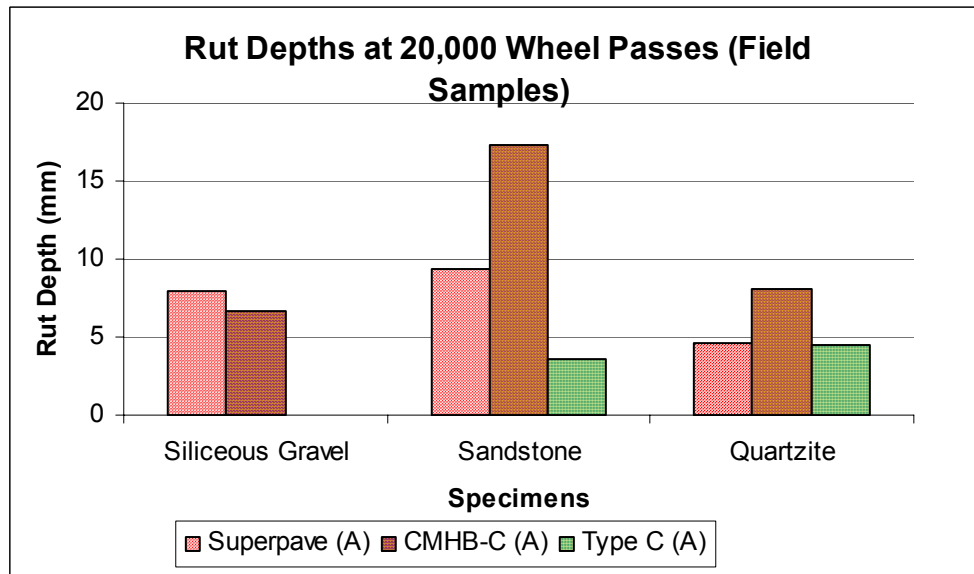


Figure A.21 Comparison of mix design effect on rut depth at 20,000 wheel passes for field samples

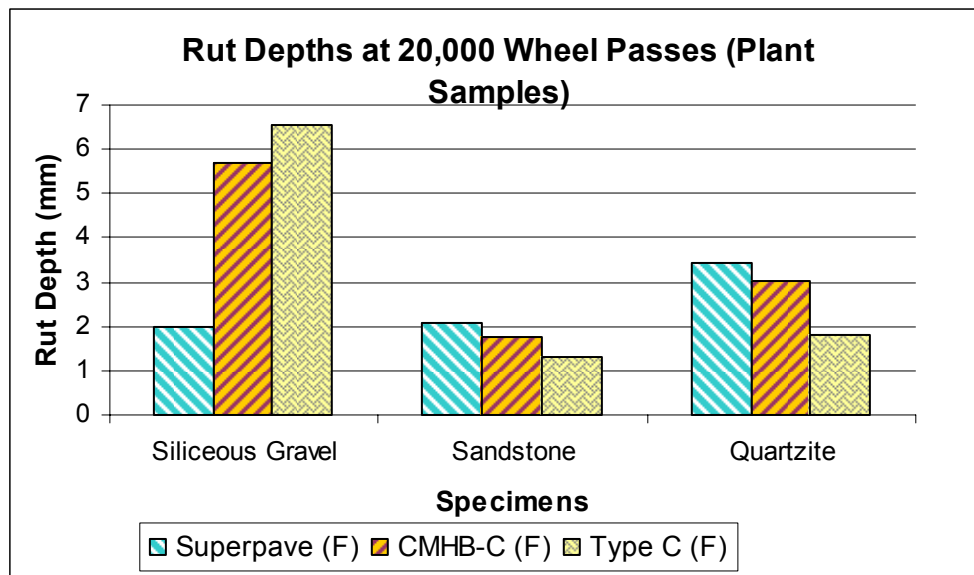


Figure A.22 Comparison of mix design effect on rut depth at 20,000 wheel passes for plant samples

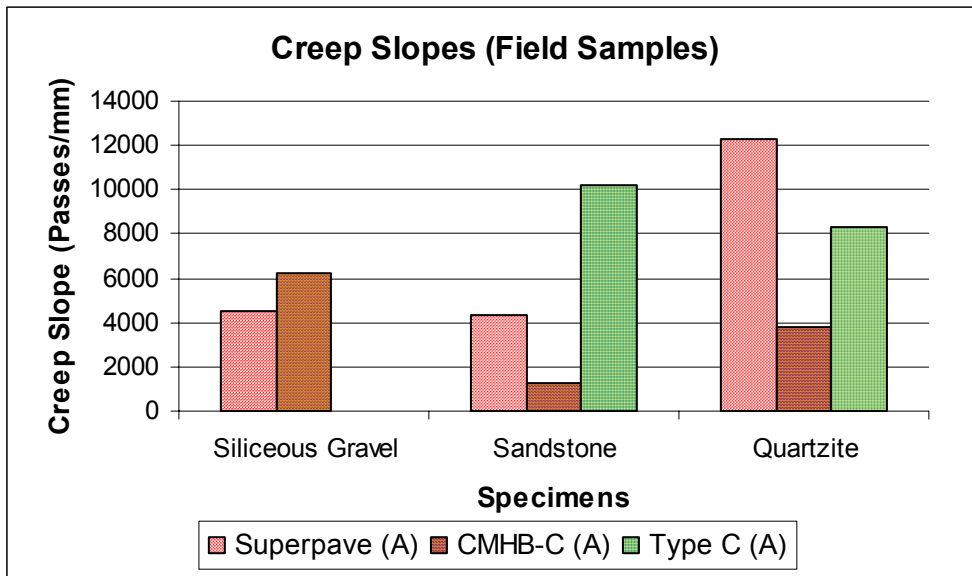


Figure A.23 Comparison of mix design effect on creep slopes for field samples

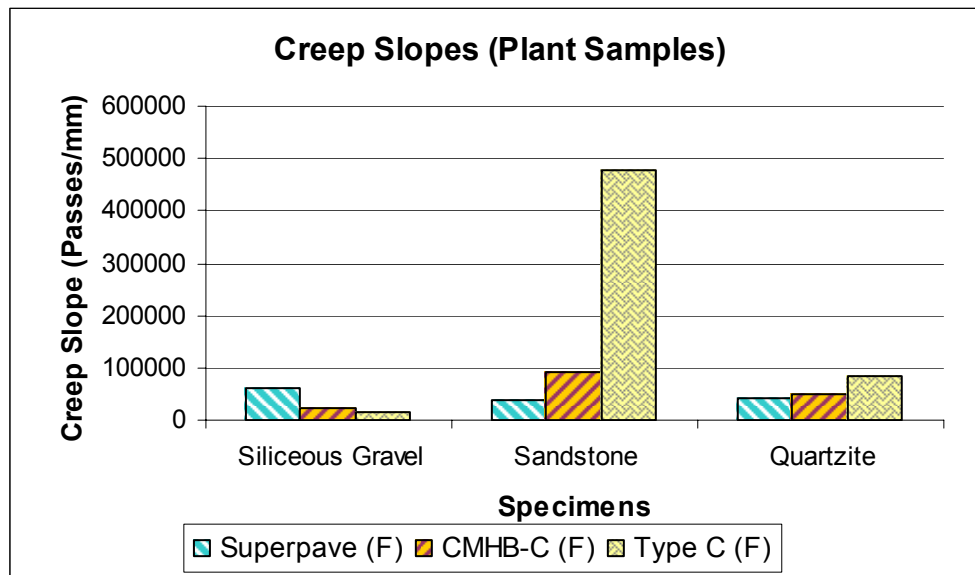


Figure A.24 Comparison of mix design effect on creep slopes for plant samples

Appendix B

Photographs of Cracks and Potholes Observed on the West Bound Outside Lane and East Bound Outside Lane



Figure B.1 Moderate transverse crack between 1305 – 1306



Figure B.2 Moderate transverse crack between 1300 – 1301



Figure B.3 Low transverse crack between 1296 – 1297



Figure B.4 Low transverse crack between 1292 – 1293



Figure B.5 Low transverse crack between 1250 – 1251



Figure B.6 Low transverse crack between 1245 – 1246



Figure B.7 Moderate transverse crack between 1234 – 1235



Figure B.8 Low transverse crack between 1228 – 1229

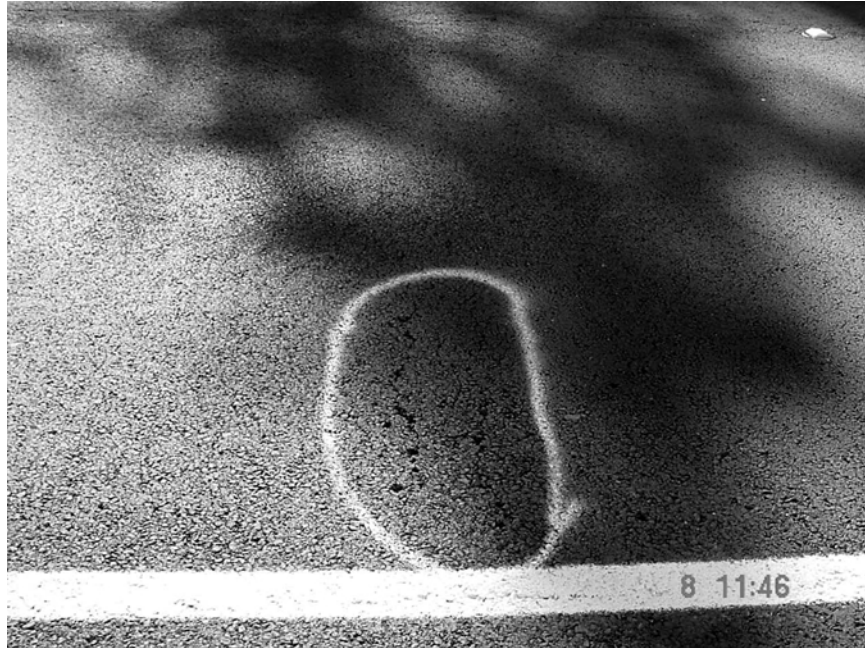


Figure B.9 Low transverse crack between 1223 – 1224



Figure B.10 Low transverse crack between 1210 – 1211



Figure B.11 Low transverse crack between 1215 – 1216



Figure B.12 Low transverse crack between 1195 – 1196



Figure B.13 Low pothole between 1150 – 1151

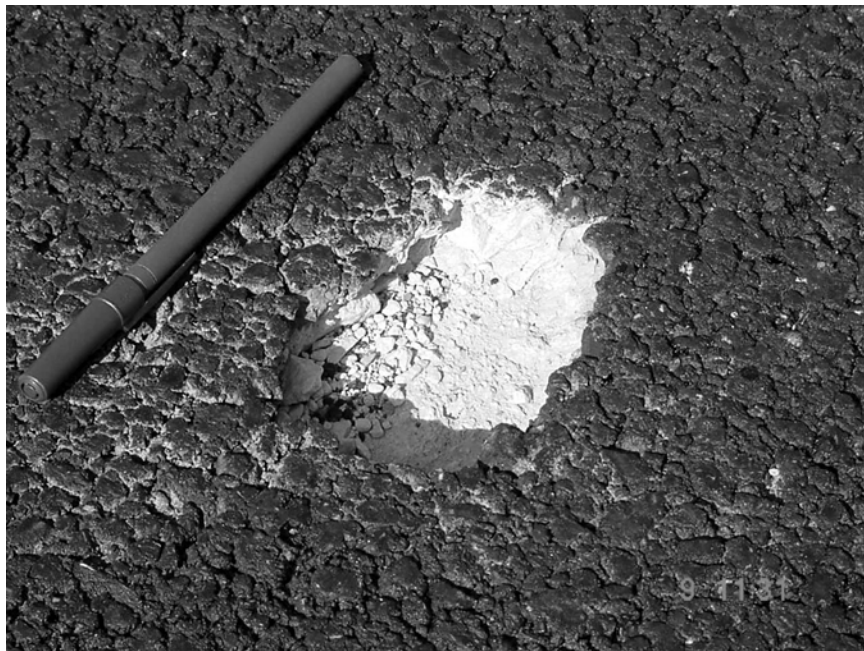


Figure B.14 Low pothole between 1249 – 1250 (Uncoated Limestone Contaminant)



Figure B.15 Low pothole between 1238 – 1239 (Underlying Concrete Failure)



Figure B.16 Low pothole between 1288 – 1289 (Uncoated Limestone Contaminant)



Figure B.17 Low transverse crack between 1292 – 1293

Appendix C

Aggregate and Mix Design Properties of the Specimens

Table C.1 Sources of the Materials Used in This Research Project

ID Marks	Mix Design	Aggregate Type	Aggregate Source	Aggregate Location
A 0111 (H 01-07)	12.5 mm Superpave	Siliceous Gravel	Hanson	Prescott
A 0112 (H 01-08)	12.5 mm Superpave	Sandstone	Meridian	Sawyer
A 0113 (H 01-09)	12.5 mm Superpave	Quartzite	Martin Marietta	Jones
A 0114 (H 01-15)	CMHB-C	Siliceous Gravel	Hanson	Prescott
A 0115 (H 01-16)	CMHB-C	Quartzite	Martin Marietta	Jones
A 0116 (H 01-17)	CMHB-C	Sandstone	Meridian	Sawyer
A 0117 (H 01-18)	Type C	Siliceous Gravel	Hanson	Prescott
A 0118 (H 01-19)	Type C	Quartzite	Martin Marietta	Jones
A 0119 (H 01-20)	Type C	Sandstone	Meridian	Sawyer
A 0120 (H 01-21)	Type B	Limestone	Hanson	Perch Hill

Table C.2 Aggregate Gradations for Superpave Mixes

Sieve Size	Cumulative Pass A0111(H01-07) Siliceous Gravel	Cumulative Pass A0112(H01-08) Sandstone	Cumulative Pass A0113(H01-09) Quartzite
19	100	100	100
12.5	92	92.1	93.7
9.5	84.8	79.4	81.7
4.75	52.4	49	45.5
2.36	30.9	29.2	31.4
1.18	20.4	22.4	21
0.6	13.9	18.9	17.7
0.3	8.8	14.9	11.8
0.15	4.5	10.2	8.2
0.075	3.2	6.5	5.6
Pan			

Table C.3 Summary of Design Mixture Properties for Superpave Mixes

ID Marks	% Air Voids	% VMA	%VFA	%G_{mm}@N_{ini}	%G_{mm}@N_{max}	DP
A 0111 (H 01-07)	3.7	15.3	73.9	86.9	97.5	0.6
A 0112 (H 01-08)	3.8	15.1	73.1	86.0	97.4	1.3
A 0113 (H 01-09)	3.8	15.6	73.1	86.5	97.4	1.1
Specifications	4.0±1.0	14.0 min	65-75	Max. 89.0	Max. 98.0	0.6-1.2

Table C.4 Aggregate Gradations for CMHB-C Mixes

Sieve Size	Cumulative Pass A0114(H01-15) Siliceous Gravel	Cumulative Pass A0115(H01-16) Quartzite	Cumulative Pass A0116(H01-17) Sandstone
7/8"	100	100	100
5/8"	99.7	99.6	100
3/8"	64.5	65.6	65.4
#4	34.3	34.2	38
#10	21.8	24	24
#40	16.2	14.5	16.4
#80	9.8	9.1	10.9
#200	6.4	5.9	6.4
pan			

Table C.5 Summary of Design Mixture Properties for CMHB-C Mixes

ID Marks	% Asphalt	% Air Voids	% VMA
A 0114 (H 01-15)	4.7	3.5	14.1
A 0115 (H 01-16)	4.8	3.5	14.6
A 0116 (H 01-17)	4.8	3.5	14.1

Table C.6 Aggregate Gradations for Type C Mixes

Sieve Size	Cumulative Pass A0117(H01-18) Siliceous Gravel	Cumulative Pass A0118(H01-19) Quartzite	Cumulative Pass A0119(H01-20) Sandstone
7/8"	100	100	100
5/8"	100	99.8	99.8
3/8"	75.8	79.1	80.7
#4	49.2	51.4	46.2
#10	31.5	34	30.9
#40	18.2	17.9	15.6
#80	11.7	10	9.6
#200	5.8	5.3	5.8

Table C.7 Summary of Stability, TSR, and HWTD Tests Results

ID Marks	Mix Design	Stability	TSR	HWTD (mm)
A 0111 (H 01-07)	12.5 mm Superpave	43	0.97	3.1
A 0112 (H 01-08)	12.5 mm Superpave	51	0.93	1.8
A 0113 (H 01-09)	12.5 mm Superpave	41	0.94	2.2
A 0114 (H 01-15)	CMHB-C	42	0.99	2.5
A 0115 (H 01-16)	CMHB-C	-	0.99	2.7
A 0116 (H 01-17)	CMHB-C	-	1.05	1.4
A 0117 (H 01-18)	Type C	48	0.96	2.5
A 0118 (H 01-19)	Type C	50	1.06	2.2
A 0119 (H 01-20)	Type C	43	0.90	1.6
A 0120 (H 01-21)	Type B	46	0.92	2.9

Appendix D

Orientation of the Test Sections

MIX DESIGN SUMMARY (SURFACE)

WEST BOUND

Table D.1 Summary of Test Section, West Bound

STATIONS	SECTION	MIX DESIGN	SY	TONS
1135 to 1188	3	SUPERPAVE ½", Quartzite Coarse Aggregate (MARTIN MARIETTA JONES MILL)	24482	2693
1193 to 1235	8	TY C, Sandstone Coarse Aggregate (MERIDIAN SAWYER)	18037	1984
1235 to 1278	5	CMHB-C, Sandstone Coarse Aggregate (MERIDIAN SAWYER)	18037	1984
1278 to 1321	2	SUPERPAVE ½", Sandstone Coarse Aggregate (MERIDIAN SAWYER)	18040	1984
SUBTOTAL			78596	8645

EAST BOUND

Table D.2 Summary of Test Section, East Bound

STATION LIMITS	SECTION	MIX DESIGN	SY	TONS
1135 to 1185	6	CMHB-C, Quartzite Coarse Aggregate (MARTIN MARIETTA JONES MILL)	15530	1708
1190 to 1218	9	TY C, Quartzite Coarse Aggregate (MARTIN MARIETTA JONES MILL)	15197	1672
1218 to 1245	1	SUPERPAVE ½", Siliceous Gravel Coarse Aggregate (HANSON EAGLE MILLS, PRESCOTT, OR LITTLE RIVER)	15956	1755
1245 to 1282	4	CMHB-C, Siliceous Gravel Coarse Aggregate (HANSON EAGLE MILLS, PRESCOTT, OR LITTLE RIVER)	15956	1755
1282 to 1321	7	TY C, Siliceous Gravel Coarse Aggregate (HANSON EAGLE MILLS, PRESCOTT, OR LITTLE RIVER)	15958	1755
SUBTOTAL			78597	8645
TOTAL			157193	17290

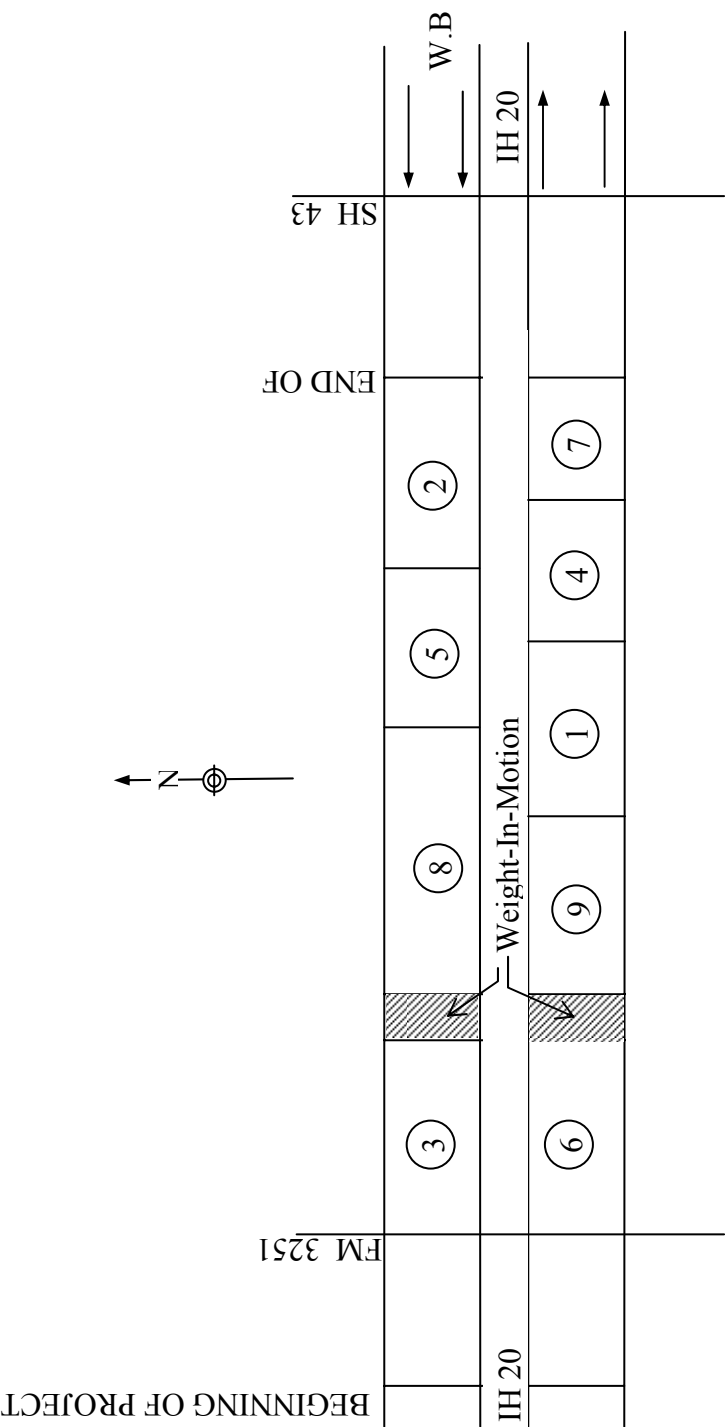


Figure D.1 Layout of the Test Sections